

# Private Iris Recognition with High-Performance FHE

Jincheol Ha\*

Cryptolab, Inc.

Seoul, Republic of Korea

Jung Hee Cheon

Cryptolab, Inc.

Seoul National University

Seoul, Republic of Korea

Guillaume Hanrot

Cryptolab, Inc.

Lyon, France

Jung Woo Kim

Cryptolab, Inc.

Seoul, Republic of Korea

Taeyeong Noh

Cryptolab, Inc.

Seoul, Republic of Korea

Damien Stehlé

Cryptolab, Inc.

Lyon, France

## Abstract

Among biometric verification systems, irises stand out because they offer both convenient capture and high accuracy even in large-scale databases of billions of users. For example, the World ID project aims to provide authentication to all humans via iris recognition, with millions already registered. Storing such biometric data raises privacy concerns, which can be addressed using privacy-enhancing cryptographic techniques.

To protect the iris codes of the database and queriers, Bloemen *et al* [IACR eprint 2024/705] describe a solution based on 2-out-of-3 Secret-Sharing Multiparty Computation (SS-MPC), for the World ID setup. The protocol takes as input iris codes of queriers and outputs bits telling if each of these codes matches a code stored in the database. In terms of security, unless an adversary corrupts 2 servers, the iris codes remain confidential and nothing leaks beyond the result of the computation. Their solution is able to match 32 users against a database of  $2^{22}$  iris codes in  $\approx 2s$ , using 24 H100 GPUs, more than 40 communication rounds and 81GB/party of data transferred (the timing assumes a network speed above 3Tb/s).

In the present work, we explore the use of Threshold Fully Homomorphic Encryption (ThFHE) for the same task. ThFHE enables arbitrary computations on encrypted data, while secret-sharing the decryption key: a given number  $t$  of decryptors among  $n$  users must collaborate to obtain the output of the computation, while  $t-1$  users cannot learn anything that is not already public. The ThFHE solution brings a number of security advantages: no trusted setup, the encrypted database and queries can be public, the parameters  $t$  and  $n$  can be increased and active security can be added without significant performance degradation.

Our proof-of-concept implementation of the computation phase handles 32 eyes against a database of  $7 \cdot 2^{14}$  iris codes in  $\approx 1.8s$  ( $\approx 0.33s$  for 4 eyes against the same database), using 8 RTX-5090 GPUs. To this, one should add 2 to 3 rounds of communication (depending on deployment choice). This gives a similar time and cost performance as the SS-MPC solution, but the saving in communication allows to maintain the performance without: 1) assuming an ultra-high-bandwidth network between non-colluding parties and 2) restricting to 2-out-of-3 security. We perform the matching using the CKKS (Th)FHE scheme. Our main technical ingredients are the use of recent progress on FHE-based linear algebra boosted using int8 GPU operations, and the introduction of a folding technique to reduce the number of ciphertexts to be processed as early as possible.

\*Corresponding author, jincheolha@cryptolab.co.kr

## Keywords

Fully Homomorphic Encryption, CKKS Scheme, Privacy-Preserving Biometrics

## 1 Introduction

Accurate biometric recognition solutions compare a query against a database of stored values that characterize legitimate users (this is often referred to as the  $1 : N$  scenario). This raises major privacy concerns: the deployment of cryptographically secure solutions is necessary not only to store such databases but also to compute on them in a privacy-preserving manner. The query deserves the same level of protection.

Among various biometric primitives (face, fingerprint, heart rhythm, etc) we choose to illustrate our approach with an iris-based biometric solution. Iris recognition offers strong accuracy even at large scale; this explains the choice of World ID to rely on it to design an authentication system for all humans. In this context, Bloemen et al. [BGK<sup>+</sup>24] use secret-sharing multiparty computation (MPC) for secure storage and recognition. More concretely, they use a protocol based on 2-out-of-3 secret sharing: 3 parties store the database shares, and 2 out of them must participate in the computation (the third party creates redundancy in case a party becomes unavailable); in terms of security, a single party has no information on the underlying data, but 2 colluding parties can reconstruct everything. Bloemen et al. [BGK<sup>+</sup>24] proposed a GPU-based implementation with impressive large-scale performance.

Secret-sharing MPC solutions, including the one from [BGK<sup>+</sup>24], suffer from several drawbacks. First, their cost scales poorly with the  $t$ -out-of- $n$  access pattern. Large values of  $t$  and  $n$  are desirable for security and robustness: a recent voting failure at the IACR showed that 3-out-of-3 secret-sharing is not robust;<sup>1</sup> further, 2-out-of-3 secret-sharing does not provide security against collusions. Second, the side-channel attack surface is large, as any party is computing on sensitive data. Third, such solutions are latency-bound, as they often require tens of communication rounds: Bloemen et al. [BGK<sup>+</sup>24] assume an NVLink between the parties, which means that they must be at same physical location, putting more stress on the no-collusion assumption of 2-out-of-3 secret sharing.

In the present work, we explore the use of threshold fully homomorphic encryption (ThFHE) [AJLA<sup>+</sup>12, BGG<sup>+</sup>18] as an alternative to secret-sharing MPC for large-scale iris recognition. ThFHE is an extension of fully homomorphic encryption (FHE) where the

<sup>1</sup>See <https://www.nytimes.com/2025/11/21/world/cryptography-group-lost-election-results.html>

decryption key is secret-shared: ThFHE involves secret-sharing aspects for key generation and decryption, but is otherwise identical to FHE. Importantly, ThFHE does not suffer from the above limitations: the main challenge is to tame its computation cost.

## 1.1 Contributions

We design and optimize a high-performance (Th)FHE protocol for iris recognition. Our proof-of-concept implementation shows that using a cluster of 8 RTX-5090 GPUs gives a match of a batch of 32 query eyes against a database of size  $7 \cdot 2^{14}$  in under 2s. The solution scales to larger databases by adding computational resources. This performance is comparable to that of [BGK<sup>+</sup>24] when taking into account the relative prices of the considered GPUs. We argue, however, that our solution has better scaling properties when one wants to further distribute security: our computation cost is almost agnostic to the number of parties involved. Further, the MPC approach requires a very large amount of communication (tenths of GB) and communication rounds (around 40) requiring ultra-high-bandwidth network for efficient deployment, while ours has low communication requirements (hundreds of KB per party) and can be deployed over WAN.

Achieving this performance requires a fast FHE library (in our case, HEaaN2 [Cry25], implementing the CKKS scheme [CKKS17]), and, crucially, the design of efficient FHE evaluation algorithms for the task at hand. The core of the iris recognition process consists in two main steps: a first step matching query data against all database entries to obtain scores with a matrix multiplication, and a second step comparing the scores to a cutoff value.

We design two homomorphic instantiations of the core computation. The first one attempts at minimizing the cost of score computation, but incurs large bootstrapping costs that dominate the overall cost. Bootstrapping [CHK<sup>+</sup>18] is a ciphertext maintenance operation that allows to continue homomorphic computations. The second one explores the idea of increasing the linear algebra costs in order to compute with scores before bootstrapping them. It leverages the ability to compute on scores to *fold* them before bootstrapping: after a small-degree polynomial evaluation, they are added by batches of size  $k$  (in our implementation, we take  $k = 16$ ) and then the sums are bootstrapped; for a large number of ciphertexts, this reduces the bootstrapping cost by a factor  $k$ .

In our implementation, we considered the very recent encrypted matrix algorithm from [BCH<sup>+</sup>25] that reduces the task to plaintext matrix multiplication. We optimized it by taking advantage of int8 tensor cores and the NVIDIA cuBLAS library.

Finally, we describe an integration of our algorithms within a larger end-to-end system for privacy-preserving iris recognition using  $t$ -out-of- $n$  ThFHE, providing high security guarantees under mild communication assumptions. This includes preprocessing the query to allow its transmission with small communication costs, and post-processing the results to enable secure threshold decryption.

## 1.2 Technical overview

We consider the core of the iris recognition process. It takes as input a database of iris templates with  $n_{\text{db}}$  entries, and a query consisting in  $\rho$  query vectors; the use of multiple query vectors (“rotations”) to encode a single query allows to compensate for

physical capture conditions. A large number of matching scores is obtained as normalized inner products of each query vector with each database entry. Each of those scores is then compared with a cutoff value, set depending on the properties of the underlying encoding. The authentication of the query user is successful if one of the resulting comparisons is positive.

**First approach.** We consider a first FHE-based approach directly following the above description. In order to minimize the linear algebra cost of the first step, we perform this computation at the smallest possible ciphertext modulus. The resulting scores are then bootstrapped so that the subsequent comparison with the cutoff can be performed homomorphically. This comparison produces  $\rho \cdot n_{\text{db}}$  matching results per query eye. Prior to recombining those results, we need to ensure that they lie in  $\{0, 1\}$ , a property which is difficult to guarantee using CKKS-based comparison when values are very close to the cutoff. We perform a *discretization* step inspired from [KN24] that forces the output to be in  $\{0, 1\}$ , allowing us to group all  $\rho \cdot n_{\text{db}}$  matching results into a single bit via an OR-tree (such binary computations can be performed in CKKS using [DMPS24, BCKS24]).

**Folding.** When handling a very large database, the main drawback of the first approach is the need to bootstrap all score values right after the score computation. This may correspond to a huge number of ciphertexts. In order to reduce the bootstrapping cost, we introduce a pretreatment of the score. This pretreatment consists in evaluating a polynomial of the score values, sending non-matching scores to small values and matching scores to large values. We build score batches of size  $k$  that contain at most one matching score; the pretreated scores in one batch can then be added while preserving the relevant information, i.e., whether this batch contains a matching score or not. This reduces the bootstrapping cost of the first method by a factor  $k$ , while increasing only moderately the pre-bootstrapping costs. We combine this folding idea with the other components of the first approach to obtain a complete chain.

**System integration.** We consider the integration of this core matching evaluation within a full system performing  $1 : N$  iris recognition. Our folding technique leads to a rather large ciphertext modulus for the query, implying a large expansion factor in communication. We describe a query format minimizing this communication cost, and a bootstrapping-based query preprocessing converting the format to the one required by the score computation. Regarding security, we rely on  $t$ -out-of- $n$  ThFHE. In order to allow for secure partial decryption, we complete the core computation chain by a high precision cleaning step [CKSS25].

## 1.3 In praise of ThFHE

The iris recognition process based on ThFHE has several advantages compared to solutions based on secret-sharing MPC.

- Most of the work, the homomorphic matching, is done on encrypted data and can hence be *performed publicly*. In particular, the encrypted database can be made public. It implies that the load can be arbitrarily distributed between computing servers. The need to trust the servers can also be decreased by adding redundancy: the computation is public and deterministic and can hence be reproduced. There is also no need to add physical protection to the servers.

- The ThFHE protocol is *communication-light*. With secret-sharing MPC, if the computing servers secret-share sensitive data and should not collude, one would prefer that they are in different physical locations, which increases communication costs. In the ThFHE protocol, there is no communication in the heavy step, unless the work is distributed on different computing servers: even in that case, as it is useless for them to collude, they can be at the same location, hence decreasing communication costs.
- *Efficiency scales well* with the number of decryptors and with an upgrade to active security: indeed, only the rather light decryption phase is impacted by an increase of the number  $n$  of users and decryption threshold  $t$ . For active security, only the partial decryptions run by the decryptors need to be strengthened by zero-knowledge proofs, the main computation remaining the same.

## 1.4 Related works

Most existing works on biometrics secured by homomorphic encryption focus on the  $1 : 1$  authentication scenario, where the user ID is provided together with the template vector, so that matching is performed against a single database entry. In this context, many papers [CCKL16, MPR20, MPR21, MPVR21, ALGRB23, MSD23, BZC<sup>+</sup>23, AB24, BHVP24, PM24, LC25, WOAS25] focus on the secure score computation and perform the comparison with the cutoff in clear, after decryption, thus disclosing some information regarding the protected data; FHE may also be combined with MPC to securely perform the comparison [BHVP24]. The best of those works typically demonstrate strong efficiency for  $1 : 1$  score computation with timings of the order of tens of milliseconds on standard CPUs, for medium template dimensions (128-512).

Some recent works explore the  $1 : N$  setting, while focusing only on score computation. In [EJB22], the authors report a performance of  $\approx 0.03$ ms per score on a 10-core CPU with template dimension 128, at the expense of a high query communication cost. The authors of [CKS<sup>+</sup>24], on the other hand, use a compact query format and report a cost of  $\approx 0.07$ ms per score computation with template dimension 128, on 8 CPU cores. Finally, FHE is combined with functional secret sharing in [IKC<sup>+</sup>24] to perform a secure comparison to the cutoff; score computation amounts to  $\approx 0.15$ ms per score for template dimension 128, on a 4-core CPU.

In addition to  $1 : N$  score computation, the authors of [ICDÖ23] also handle the comparison step homomorphically. To scale to medium-sized databases, they introduce a group testing idea which bears resemblance to our *folding* approach, by computing a somewhat heuristic approximation of the maximum of a number of scores; the heuristic nature of the approximation leads to a rather high rate of false rejections. Using somewhat homomorphic encryption, they process  $2^{14}$  scores in template dimension 128 in  $\approx 9.4$ s on one CPU.

## 2 Preliminaries

We use boldface letters for matrices and vectors. We let the integer ring be denoted by  $\mathbb{Z}$  and the field of real (resp. complex) numbers by  $\mathbb{R}$  (resp.  $\mathbb{C}$ ). The sets  $\mathbb{R}^n$  and  $\mathbb{C}^n$  are equipped with their coordinate-wise ring structure, with multiplication denoted

by  $\odot$ . We let  $\|\cdot\|_1$  denote the  $L^1$ -norm, i.e.,  $\|\mathbf{x}\|_1 = \sum_{i=0}^{n-1} |x_i|$  for  $\mathbf{x} \in \mathbb{R}^n$ . For  $x \in \mathbb{R}$ , we define  $\lfloor x \rfloor = \lfloor x + 1/2 \rfloor$ , where  $\lfloor \cdot \rfloor$  refers to the integer part. The notation  $\log$  refers to the base-2 logarithm. Finally, we use  $\wedge$ ,  $\vee$  and  $\oplus$  for the and, or and xor boolean operators, respectively, and let them operate coordinate-wise on vectors.

## 2.1 Plain iris recognition

In this section, we summarize the iris recognition process proposed by Daugman [Dau04]. The first step is image segmentation, converting an input iris image into two binary vectors of the same size: an *iris code*  $\mathbf{c} \in \{0, 1\}^\ell$  obtained by segmenting and normalizing the input iris image, and a *mask*  $\mathbf{m} \in \{0, 1\}^\ell$  used to occlude non-iris parts of  $\mathbf{c}$  such as eyelids and eyelashes in the iris image. A pair of an iris code and a corresponding mask is called *iris template*. Daugman used 2-dimensional Gabor wavelets for this iris image processing, and the World ID infrastructure used machine learning techniques for more precise image processing. We omit the details for this part and assume an iris template  $(\mathbf{c}, \mathbf{m})$  is given as input.

**2.1.1 Distance on iris templates.** Given an iris template  $(\mathbf{c}, \mathbf{m})$ , the usable iris part from the original iris image corresponds to  $\mathbf{c} \wedge \mathbf{m} \in \{0, 1\}^\ell$ . For a pair of iris templates  $((\mathbf{c}_1, \mathbf{m}_1), (\mathbf{c}_2, \mathbf{m}_2))$ , the componentwise AND  $\mathbf{m}_1 \wedge \mathbf{m}_2$  denotes the overlapped iris area. The distance between two iris templates is defined as:

$$\begin{aligned} \text{dist}((\mathbf{c}_1, \mathbf{m}_1), (\mathbf{c}_2, \mathbf{m}_2)) &= \frac{\text{hd}(\mathbf{c}_1 \wedge \mathbf{m}_1, \mathbf{c}_2 \wedge \mathbf{m}_2)}{\|\mathbf{m}_1 \wedge \mathbf{m}_2\|_1} \\ &= \frac{\langle \mathbf{c}_1 \oplus \mathbf{c}_2, \mathbf{m}_1 \wedge \mathbf{m}_2 \rangle}{\|\mathbf{m}_1 \wedge \mathbf{m}_2\|_1} \end{aligned} \quad (1)$$

where the Hamming distance  $\text{hd}$  between two binary vectors  $\mathbf{x}$  and  $\mathbf{y}$  is defined by  $\text{hd}(\mathbf{x}, \mathbf{y}) = \|\mathbf{x} \oplus \mathbf{y}\|_1$ .

If either iris code  $\mathbf{c}_1$  or  $\mathbf{c}_2$  is a uniform binary vector independent of the other one, then  $\mathbf{c}_1 \oplus \mathbf{c}_2$  is expected to behave as a uniform binary vector, so that the distance is close to  $1/2$ . Daugman found that two eyes of different individuals and also different eyes of the same individual have independent behavior, obtaining a close-to-normal distribution centered near  $1/2$  for the distance between the iris templates. Conversely, if the iris templates are obtained from the same eye so that they are close to each other, then the distance would be close to 0. By using this difference between the matching case (i.e., iris templates from the same eye) and the non-matching case, we can decide whether two iris templates come from the same eye or not. But even for the same eye, obtaining close iris templates is not easy in the real world because we cannot ideally reproduce the same environment when taking the iris images.

**2.1.2 Iris template rotations.** To mitigate the issue above, one of the iris templates to be matched is rotated (both code and mask) by a small offset several times, and the distance to the other one is computed independently for all rotations. If the irises are independent, the rotations do not affect the distribution of the distance (Daugman experimentally showed that they can be assumed independent). On the other hand, when considering the same eye, we can expect that at least one of the rotations would result in a small distance (the distance from the other rotations may give a larger distance as in the non-matching case). Hence, by taking the minimum distance among different rotations, one can compensate for the non-ideal physical measurement of the iris image.

Now, we can choose a cutoff  $t \in (0, 1)$  and decide that two iris codes come from the same eye when the minimum distance among rotated iris codes is smaller than  $t$ . A larger  $t$  is more likely to result in incorrect matching (false positive), while a smaller  $t$  is more likely to result in incorrect non-matching (false negative).

**2.1.3 Masked bitvector representation.** To compute the distance more efficiently, Bloemen et al. [BGK<sup>+</sup>24] adopted a masked bitvector representation as follows. Given two iris data  $(\mathbf{c}_i, \mathbf{m}_i) \in \{0, 1\}^{\ell}$  for  $i \in \{1, 2\}$ , define a ternary vector  $\mathbf{c}'_i$  by

$$\mathbf{c}'_i = \mathbf{m}_i - 2 \cdot (\mathbf{c}_i \wedge \mathbf{m}_i) \in \{-1, 0, 1\}^{\ell}.$$

Then, we have  $2 \cdot \langle \mathbf{c}_1 \oplus \mathbf{c}_2, \mathbf{m}_1 \wedge \mathbf{m}_2 \rangle = \|\mathbf{m}_1 \wedge \mathbf{m}_2\|_1 - \langle \mathbf{c}'_1, \mathbf{c}'_2 \rangle$ , so that we can replace the matching decision criteria by

$$\frac{\langle \mathbf{c}'_1, \mathbf{c}'_2 \rangle}{\|\mathbf{m}_1 \wedge \mathbf{m}_2\|_1} > 1 - 2t. \quad (2)$$

In this work, we call the left side of (2) the *score* of the iris pair.

**2.1.4 Homomorphic context and database matching.** In the context of homomorphic evaluation, implementing a decision criterion like (2) is not feasible efficiently. Rather, we assume that we are given two intervals  $\mathcal{N} = [s, t_0]$  and  $\mathcal{P} = [t_1, u]$  with  $t_0 < t_1$  such that all scores belong to  $[s, u]$ , and we implement the following:

$$\begin{aligned} \frac{\langle \mathbf{c}'_1, \mathbf{c}'_2 \rangle}{\|\mathbf{m}_1 \wedge \mathbf{m}_2\|_1} \in \mathcal{N} &\Rightarrow \text{Return false ,} \\ \frac{\langle \mathbf{c}'_1, \mathbf{c}'_2 \rangle}{\|\mathbf{m}_1 \wedge \mathbf{m}_2\|_1} \in \mathcal{P} &\Rightarrow \text{Return true .} \end{aligned} \quad (3)$$

In the case where the score is in  $(t_0, t_1)$ , we consider the output to be unspecified but it should be either true or false, to allow further computations that assume the result is binary. We let the result of this operation be denoted by  $\text{match}(\mathbf{c}_1, \mathbf{m}_1), (\mathbf{c}_2, \mathbf{m}_2)$ .

For the matching of a set of iris templates for rotations of a fixed iris  $\mathbf{C}^{(\text{qry})} = (\mathbf{c}_r^{(\text{qry})}, \mathbf{m}_r^{(\text{qry})})_{0 \leq r < \rho}$  against a whole database of iris templates  $\mathbf{C}^{(\text{db})} = (\mathbf{c}_i^{(\text{db})}, \mathbf{m}_i^{(\text{db})})_{0 \leq i < n_{\text{db}}}$ , we define:

$$\text{match}_{\text{db}}(\mathbf{C}^{(\text{qry})}, \mathbf{C}^{(\text{db})}) = \bigvee_{\substack{0 \leq i < n_{\text{db}} \\ 0 \leq r < \rho}} \text{match} \left( (\mathbf{c}_r^{(q)}, \mathbf{m}_r^{(q)}), (\mathbf{c}_i^{(\text{db})}, \mathbf{m}_i^{(\text{db})}) \right).$$

## 2.2 CKKS

Compared to other FHE schemes, CKKS handles complex numbers as cleartexts rather than elements of finite fields (as BFV [Bra12, FV12] and BGV [BGV14]) or small integers (as TFHE [CGGI20]). It is, by construction, an approximate system, providing operations on cleartexts with a precision that can be parameterized.

Below, we provide a brief description of elementary CKKS operations. More CKKS background, on bootstrapping, ring-packing and the use of the maximal real subfield is provided in Appendix A.

**2.2.1 Encoding and decoding.** Let  $N$  be a power-of-two integer. The message ring is  $(\mathbb{C}^{N/2}, +, \odot)$ , and the plaintext space is the ring  $\mathcal{R} = \mathbb{Z}[X]/(X^N + 1)$ . CKKS uses two encoding maps  $\text{Ecd}_{\text{slot}}$ ,  $\text{Ecd}_{\text{coeff}}$  :  $(x_i)_{0 \leq i < N/2} \mapsto [\Delta P]$  for a scaling factor  $\Delta$  and where  $P$  is respectively defined by  $P(\zeta^{5^i}) = x_i$  for  $0 \leq i < N/2$  and  $P = \sum_{i=0}^{N/2-1} (\text{Re}(x_i) + \text{Im}(x_i)X^{N/2}) \cdot X^i$ . The scaling factor  $\Delta$  controls the level of discretization: the larger  $\Delta$ , the higher the precision.

The approximate identities

$$\begin{aligned} \text{Ecd}_{\text{slot}}(\mathbf{u} + \mathbf{v}) &\approx \text{Ecd}_{\text{slot}}(\mathbf{u}) + \text{Ecd}_{\text{slot}}(\mathbf{v}) \\ \text{Ecd}_{\text{slot}}(\mathbf{u} \odot \mathbf{v}) &\approx \Delta^{-1} \cdot \text{Ecd}_{\text{slot}}(\mathbf{u}) \odot \text{Ecd}_{\text{slot}}(\mathbf{v}) \end{aligned}$$

show that through CKKS encoding the arithmetic of the plaintext space corresponds to the arithmetic of the message ring. In the sequel, we shall write  $\text{Ecd}$  for  $\text{Ecd}_{\text{slot}}$  and  $\text{Dcd}$  (resp.  $\text{Dcd}_{\text{coeff}}$ ) for the inverse map of  $\text{Ecd}$  (resp.  $\text{Ecd}_{\text{coeff}}$ ), up to rounding. In the case of  $\text{Ecd}_{\text{slot}}$ , each coordinate of the message vector is called a slot.

**2.2.2 Ciphertexts.** CKKS relies on the RLWE problem [SSTX09, LPR10]. Its secret key  $\text{sk}$  lies in  $\mathcal{R}$  and its public key and ciphertexts are pairs  $\text{ct} = (a, b)$  of elements in  $\mathcal{R}_Q = \mathbb{Z}_Q[X]/(X^N + 1)$ . Decryption is defined as  $\text{Dec}_{\text{sk}}((a, b)) = a \cdot \text{sk} + b$ , whereas encryption takes as input a plaintext  $P$  and a public key, and returns a ciphertext  $(a, b)$  such that  $a \cdot \text{sk} + b \approx P$ . We refer to [CKKS17] for key generation and the description of encryption.

**2.2.3 Operations.** CKKS provides the following operations:

- Add. On input  $\text{ct} = (a, b)$ ,  $\text{ct}' = (a', b')$ , return  $(a + a', b + b')$ ; one then has  $\text{Dec}(\text{Add}(\text{ct}, \text{ct}')) = \text{Dec}(\text{ct}) + \text{Dec}(\text{ct}')$ .
- Mult. On input  $\text{ct} = (a, b)$ ,  $\text{ct}' = (a', b')$ , and a relinearization key  $\text{relk}$ , return a ciphertext  $\text{Mult}(\text{ct}, \text{ct}')$  that decrypts then decodes to  $\approx \text{Dcd}(\text{Dec}(\text{ct})) \odot \text{Dcd}(\text{Dec}(\text{ct}'))$ ;  $\text{Mult}$  can be specialized to a more efficient version for handling products of a plaintext by a ciphertext.
- Rot. On input  $\text{ct} = (a, b)$  encrypting  $(x_i)_{0 \leq i < N/2}$ , an integer  $0 \leq \ell < N/2$  and an associated key  $\text{rotk}_{\ell}$ , return a ciphertext  $\text{Rot}_{\ell, \text{rotk}_{\ell}}(\text{ct})$  that decrypts then decodes to  $\approx (x_{i+\ell \bmod N/2})_{0 \leq i < N/2}$ .

Based on addition and multiplication, one can perform slot-wise polynomial evaluation. The cost of the Paterson-Stockmeyer algorithm [PS73] is dominated by  $O(\sqrt{d})$  ciphertext-ciphertext multiplications, where  $d$  is the polynomial degree.

**2.2.4 Maintenance.** When multiplying two encoded plaintext with scaling factor  $\Delta$ , one obtains a plaintext encoded with scaling factor  $\Delta^2$ . In order to preserve the scaling factor, a division by  $\Delta$  is required. This is realized, for  $(a, b) \in R_Q^2$  and  $\Delta | Q$ , as

$$\text{Rescale}_{\Delta}((a, b)) = \left( \left\lfloor \frac{a}{\Delta} \right\rfloor, \left\lfloor \frac{b}{\Delta} \right\rfloor \right) \bmod \frac{Q}{\Delta}.$$

In practice, one uses  $\text{Rescale}_q$  for  $q \approx \Delta$ , so that different  $q$ 's may be used for the same  $\Delta$  while allowing RNS arithmetic for ciphertexts.

Rescale leads to a reduction of the ciphertext modulus: during a computation, the modulus decreases with multiplications. This reduction is proportional to  $\Delta$ , which controls the precision of the computation: modulus loss is directly related to precision needs. In a simplified view, one can assume that modulus can only take a finite number of values  $Q_L > Q_{L-1} > \dots > Q_0$ ; in that case, we refer to the *level* of a ciphertext in  $[0, L]$  rather than to its modulus.

When modulus becomes low, the ciphertext must be refreshed via bootstrapping (BTS) [CHK<sup>+</sup>18]. As bootstrapping is costly, designers of homomorphic algorithms try to reduce the number of bootstraps as much as possible, by a tight control on the modulus used by the computations. Homomorphic algorithm design targets a sharp control of multiplicative depth and plaintext precision.

### 2.3 Linear algebra in CKKS

The start of the iris recognition computation is a matrix-matrix product, where both operands are encrypted (CCMM). We focus on the RGSW-based approach described in [BCH<sup>+</sup>25]. We summarize here the properties required for the description of our contributions. We make extensive use of the MSRLWE (also known as “shared-a”) ciphertext format as in [BCH<sup>+</sup>24, BCH<sup>+</sup>25]; in the case of large matrices, using this format reduces both the memory footprint and the computational cost. When used to multiply a large preprocessed database  $\mathbf{M}_{\text{db}}$  of dimension  $d_1 \times d_2$  by a query  $\mathbf{M}_{\text{qry}}$  of dimensions  $d_2 \times d_3$ , using scaling factor  $\Delta$ , and ring degrees  $N_{\text{db}}$  and  $N_{\text{qry}}$  for the encryption layer of  $\mathbf{M}_{\text{db}}$  and  $\mathbf{M}_{\text{qry}}$ :

- the encrypted  $\mathbf{M}_{\text{db}}$  is represented by four matrices modulo an integer  $\approx Q^2/\Delta$  of respective dimensions  $N_{\text{db}} \times d_2$ ,  $d_1 \times d_2$ ,  $N_{\text{db}} \times N_{\text{qry}}$  and  $d_1 \times N_{\text{qry}}$ ; here, we complete the database with zero entries so that  $N_{\text{db}} \mid d_1$ , and pad each database entry with zeroes so that  $N_{\text{qry}} \mid d_2$ ;
- the encrypted query  $\mathbf{M}_{\text{qry}}$  is represented by two matrices modulo  $Q$  of respective dimensions  $N_{\text{qry}} \times d_3$  and  $d_2 \times d_3$ ;
- the result  $\mathbf{M}_{\text{db}} \cdot \mathbf{M}_{\text{qry}}$  is represented by two matrices modulo an integer  $\approx Q/\Delta$  of dimensions  $N_{\text{db}} \times d_3$  and  $d_1 \times d_3$ ; the second matrix corresponds to  $d_1 d_3 / N_{\text{db}}$  ciphertexts with ring-degree  $N_{\text{db}}$  and modulus  $\approx Q/\Delta$ ; each ciphertext encrypts  $N_{\text{db}}$  consecutive coefficients of one column of  $\mathbf{M}_{\text{db}} \cdot \mathbf{M}_{\text{qry}}$ ;
- the computation is dominated by four plaintext matrix-matrix products modulo an integer  $\approx Q^2/\Delta$ .

We let this algorithm be denoted by  $\text{CCMM}(\widehat{\mathbf{M}_{\text{db}}}, \widehat{\mathbf{M}_{\text{qry}}})$ , where  $\widehat{\mathbf{M}_{\text{db}}}$  and  $\widehat{\mathbf{M}_{\text{qry}}}$  are the encryptions of  $\mathbf{M}_{\text{db}}$  and  $\mathbf{M}_{\text{qry}}$ , respectively. It was designed to multiply encrypted matrices with coefficient-encoded messages, and return an encrypted matrix with coefficient-encoded messages. It is however compatible with  $\mathbf{M}_{\text{db}}$  using slot-encoding and  $\mathbf{M}_{\text{qry}}$  using coefficient-encoding. A similar situation is discussed in [BCH<sup>+</sup>24]. Conversely, the algorithm is also able to handle a slot-encoded  $\mathbf{M}_{\text{db}}$  by replacing  $\mathbf{M}_{\text{db}}$  by  $\mathbf{M}_{\text{db}} \cdot \mathbf{M}_{\text{Cts}}$ , where  $\mathbf{M}_{\text{Cts}}$  is the Cts matrix for ring degree  $N_{\text{qry}}$  (see [CHK<sup>+</sup>18]). In all cases, the encoding type of the result is that of  $\mathbf{M}_{\text{db}}$ .

### 2.4 Two-way classification in CKKS

Let  $I_0, I_1$  be two disjoint intervals and  $\varepsilon > 0$ . We say that  $\text{cl} : \mathbb{R} \rightarrow \mathbb{R}$  is an  $(I_0, I_1, \varepsilon)$ -classification function if  $|\text{cl}(x) - b| \leq \varepsilon$  when  $x \in I_b$ , for  $b \in \{0, 1\}$ ; the behavior of  $\text{cl}$  outside of  $I_0 \cup I_1$  is unspecified, but in this paper we only consider realizations such that  $\text{cl}(x) \in [-\varepsilon, 1 + \varepsilon]$  for  $x$  in the convex hull of  $I_0 \cup I_1$ . We use this classification primitive for implementing (3) and for making imprecise approximations to binary values  $\{0, 1\}$  more precise (both for correctness and for threshold decryption security). In CKKS, approximate classification functions are constructed using polynomials. In the sequel, we write  $\text{Classify}_\varepsilon(I_0, I_1, \text{ct})$  for the homomorphic evaluation of an  $(I_0, I_1, \varepsilon)$ -classification function on entry  $\text{ct}$ . For very small  $\varepsilon$ , we make use of the solution described in [CKSS25, Figure 2], to lower modulus usage towards the end of the computation. Borrowing from the terminology introduced in [DMPS24], we shall call *cleaning* this specific classification regime.

Except in situations where the relative gap is large, classification is a deep operation and requires prior bootstrapping in order to restore a sufficiently large modulus.

We refer to Appendix B for more details on the implementation of classification in CKKS.

### 3 A first algorithm

For the sake of simplicity, throughout Sections 3 and 4, we assume that the embedding dimension  $d$  of the iris codes coincides with the CKKS ring degree  $N$ , and that the latter is the same for all ciphertexts; this is not required for the implementation described in Section 6.

We now describe a first approach to homomorphically evaluate the iris recognition algorithm. We assume that we are provided the CKKS-encrypted database of the iris codes  $(\mathbf{c}_k^{(\text{db})})_{0 \leq k < n_{\text{db}}}$  of the registered users. When the encrypted query is received, the goal is to assess whether the query eye is registered in the database or not: this corresponds to the evaluation of the  $\text{match}_{\text{DB}}$  primitive defined in Section 2.1. We consider the following steps.

- (1) [Query preprocessing] Given an encrypted query in a format minimizing communication, turn the query into a suitable format for score computation.
- (2) [Batched inner products computation] Compute the inner products by CCMM; these are the numerators of the scores.
- (3) [Normalize] Divide the inner product outputs by the denominators to obtain the scores.
- (4) [Classify] Turn the scores in the union of intervals  $\mathcal{N} \cup \mathcal{P}$  into values in  $\{0, 1\}$  by evaluating a classification function; scores outside  $\mathcal{N} \cup \mathcal{P}$  are sent to  $(0, 1)$ .
- (5) [Result post-processing] Send values in  $(0, 1)$  to  $\{0, 1\}$  and group them into a single bit.

Step 3 is performed using plaintext-ciphertext multiplications, where the plaintexts store the inverses of the denominators. Step 4 is handled using the strategy outlined in Appendix B. We describe the details of the other steps in the following subsections. The full algorithmic description is given as Algorithm 1.

#### 3.1 Query transmission and preprocessing

A query for an eye consists of  $\rho$  rotated iris codes  $(\mathbf{c}_r^{(\text{qry})})_{0 \leq r < \rho} \in \{0, 1\}^d$ , together with the associated masks. In the present work, we consider that only the former are encrypted, and thus restrict the discussion of packing and transmission to the iris codes.

**3.1.1 Query representation.** To reduce both communication and bootstrapping costs, we assume that the encrypted queries are sent using the smallest possible ciphertext modulus  $q_0 \approx 2^\delta$ . For this purpose, we use coefficient encoding and place the plaintext in the most significant bits of ciphertexts as suggested in [BCKS24, Section 6]. Such a query can be represented as  $\rho$  ciphertexts  $(\mathbf{ct}_i^{(\text{qry})})_{0 \leq i < \rho}$  in  $\mathcal{R}_{q_0, N}^2$ , leading to an expansion factor of  $\approx 2\delta$ . This expansion factor is improved by packing bits into small integers before encrypting them. If  $1 < \beta \leq \rho$  is an integer packing parameter, the query can be represented as  $\mathbf{ct}'_j = \sum_{i=0}^{\beta-1} 2^i \mathbf{ct}_{j\beta+i}^{(\text{qry})}$ , for  $0 \leq j < \lceil \rho/\beta \rceil$ . This requires increasing the modulus from  $\delta$  to  $\delta + \beta$  bits, but overall reduces the expansion factor by a factor  $\approx (\delta + \beta)/(\delta\beta)$ .

---

**Algorithm 1** Iris recognition, first algorithm – case of a single query, of embedding dimension matching the CKKS ring degree

---

**Require:** Parameters  $\mathcal{N}, \mathcal{P}, \varepsilon_0, \Delta, \delta, \mathcal{N}', \mathcal{P}', \varepsilon_1$ ; ring degree  $N$ .  
**Require:**  $(\widehat{\mathbf{M}_{\text{db}}}, \mathbf{m}^{(\text{db})})$  a database of  $n_{\text{db}}$  irises where  $\widehat{\mathbf{M}_{\text{db}}}$  is a (collection of) ciphertext(s) in CCMM-compatible encrypted format with ring-degree  $N$  dividing  $n_{\text{db}}$ , along with the corresponding masks.  
**Require:**  $(\mathbf{ct}_r^{(\text{qry})}, \mathbf{m}_r^{(\text{qry})})_{0 \leq r < \rho}$ , a vector of query ciphertexts and masks.  
**Ensure:** Ciphertext  $\mathbf{ct}_{\text{out}}$  encrypting a single bit corresponding to the  $\text{match}_{\text{db}}$  function applied to the inputs.

```

 $\widehat{\mathbf{M}_{\text{qry}}} \leftarrow \text{QueryPreprocess}((\mathbf{ct}_r^{(\text{qry})})_{0 \leq r < \rho})$ 
 $(\mathbf{ct}_r^{(\ell)})_{0 \leq r < \rho, 0 \leq \ell < n_{\text{db}}/N} \leftarrow \text{CCMM}(\widehat{\mathbf{M}_{\text{db}}}, \widehat{\mathbf{M}_{\text{qry}}})$ 
 $\mathbf{ct}_{\text{out}} \leftarrow (0, 0)$ 
/* main loop */
for  $0 \leq \ell < n_{\text{db}}/N$  do
  for  $0 \leq r < \rho$  do
     $\mu_r^{(\ell)} \leftarrow \text{Ecd}((\|\mathbf{m}_r^{(\text{qry})} \wedge \mathbf{m}_j^{(\text{db})}\|_1^{-1})_{N\ell \leq j < N(\ell+1)-1})$ 
     $\mathbf{ct}_r^{(\ell)} \leftarrow \mathbf{ct}_r^{(\ell)} \odot \mu_r^{(\ell)}$ 
     $\mathbf{ct}_r^{(\ell)} \leftarrow \text{Classify}_{\varepsilon_0, \mathcal{N}, \mathcal{P}}(\mathbf{ct}_r^{(\ell)})$ 
     $\mathbf{ct}_r^{(\ell)} \leftarrow \text{BTS}(\text{Rescale}_{\Delta/2^\delta}(\mathbf{ct}_r^{(\ell)}))$ 
     $\mathbf{ct}_{\text{out}} \leftarrow \mathbf{ct}_{\text{out}} \vee \text{Classify}_{\varepsilon_1, \mathcal{N}', \mathcal{P}'}(\mathbf{ct}_r^{(\ell)})$ 
  end for
end for
/* end of main loop */
for  $i$  from  $0$  to  $\log N - 1$  do
   $\mathbf{ct}_{\text{out}} \leftarrow \mathbf{ct}_{\text{out}} \vee \text{Rot}_{2^i}(\mathbf{ct}_{\text{out}})$ 
end for
return  $\mathbf{ct}_{\text{out}}$ 

```

---

**3.1.2 Query preprocessing.** The query is in a format that is unsuitable for direct homomorphic computations, its packing format being inadequate if  $\beta > 1$  and, more generally, its modulus and precision being intentionally chosen very small to minimize communication costs. The following preprocessing steps are thus performed on the query, in order to prepare it for the linear algebra step:

- Integer bootstrapping and bit extraction [BKSS24], in order to raise ciphertext modulus and unpack the small integers into bits; depending on the value of  $N$ , this step may require applying ring-packing to the query to obtain a ring degree for which bootstrapping is possible.
- Increasing the precision of the bits (see Section 2.4).
- Conversion to the masked bit-vector representation (see Section 2.1.3). Since  $\mathbf{m} - 2 \cdot (\mathbf{c} \wedge \mathbf{m}) = \mathbf{m} \odot (1 - 2 \cdot \mathbf{c})$ , this step consumes a plaintext-ciphertext multiplication.

The cost of bit extraction growing quickly with  $\beta$ , we apply the packing strategy to small values of  $\beta$ .

## 3.2 Scores computation

The iris scores are computed as the inner products  $\langle \mathbf{c}_k^{(\text{db})}, \mathbf{c}_r^{(\text{qry})} \rangle$ , for  $0 \leq k < n_{\text{db}}$ ,  $0 \leq r < \rho$ . This is viewed as the computation of a product of two encrypted matrices  $\mathbf{M}_{\text{db}}$  and  $\mathbf{M}_{\text{qry}}$ , for which we use the algorithm discussed in Section 2.3.

The use of this CCMM algorithm creates a number of implementation constraints; in particular, in order to obtain the scores as ciphertexts modulo  $Q$ , the database has to be represented as a ciphertext with modulus  $Q^2/\Delta$ . This roughly doubles the cost of the linear algebra computation, but also the storage size of the database. In order to keep both small, the natural strategy is to perform the CCMM computation at the smallest possible modulus. This produces  $\rho \cdot n_{\text{db}}$  scores at a low ciphertext modulus, leading to the requirement to bootstrap all these scores. For a large database, the number of ciphertexts  $\rho \cdot n_{\text{db}}/N$  can be high.

## 3.3 Scores post-processing

Once the scores have been computed, a post-treatment is required in order to only return relevant information, i.e., the value of  $\text{match}_{\text{db}}$ . The first step of this post-treatment is a classification, implementing (3), and returning values in  $[0, 1]$  that are close to 0 (resp. 1) for scores in  $\mathcal{N}$  (resp.  $\mathcal{P}$ ). This implements the  $\text{match}$  function.

Biometrics inaccuracies and rotations of a match may lead to scores that are outside  $\mathcal{N} \cup \mathcal{P}$ . In this case, classification may output values strictly between 0 and 1. This is inconvenient for the OR tree. To handle this difficulty, we use a discretization step that sends any value from  $(0, 1)$  to either 0 or 1. Through this process, the biometrics inaccuracies may lead to false positives and false negatives, which is unavoidable given the input data. In the case of rotations of a valid query, one of the rotations is expected to output 1, so the others do not impact the result of the OR tree.

**3.3.1 Discretization.** Let  $(v_0, \dots, v_{N-1}) \in [0, 1]^N$  be  $N$  results of the  $\text{match}$  function applied to query and database irises – most of them are expected to be very close to 0 or 1 but some may be in-between. Assume a ciphertext  $(a, b)$  encrypts  $(v_i)_{0 \leq i < N}$  under  $\text{sk}$  in coefficient encoding at modulus  $q_0$ , with scaling factor  $2^\delta$ , i.e.:

$$a \cdot \text{sk} + b = \sum_{i=0}^{N-1} (2^\delta v_i + e_i) X^i \bmod q_0 ,$$

where  $e_i$  accounts for the overall (computational and cryptographic) error; we assume that  $|e_i| \leq e_{\text{comp}}$  for all  $i$ . We observe in particular that  $2^\delta v_i + e'_i$  is an integer in  $[-q_0/2, q_0/2]$ .

We half-bootstrap this ciphertext, which produces a slot-encoded ciphertext and introduces a slot- $i$  error  $\varepsilon_i$  with  $\max_i |\varepsilon_i| \leq e_{\text{bts}}$ , giving a value  $2^\delta v_i + e'_i + \varepsilon_i$ . We then have the following properties:

- Values  $v_i = 0$  (resp.  $v_i = 1$ ) are mapped to  $\mathcal{N}' = [-e_{\text{comp}} - e_{\text{bts}}, e_{\text{comp}} + e_{\text{bts}}]$  (resp.  $\mathcal{P}' = [2^\delta - e_{\text{comp}} - e_{\text{bts}}, 2^\delta + e_{\text{comp}} + e_{\text{bts}}]$ ); when bootstrapping precision is sufficient,  $e_{\text{comp}} + e_{\text{bts}}$  is small compared to  $2^\delta$ , and  $\mathcal{N}'$  and  $\mathcal{P}'$  are disjoint.
- The slot values after half-bootstrapping lie within  $e_{\text{bts}}$  of the integer value  $2^\delta v_i + e'_i$ .

Let  $n' = \lceil \max \mathcal{N}' \rceil$  and  $p' = \lfloor \min \mathcal{P}' \rfloor$ . For well-chosen parameters, we have  $n' < p'$ . We choose an integer  $\tau \in (n', p']$  and evaluate an  $([\min \mathcal{N}', \tau - 1 + e_{\text{bts}}], [\tau - e_{\text{bts}}, \max \mathcal{P}'], \varepsilon)$ -classification function, obtaining a result that lies within  $\varepsilon$  of  $\{0, 1\}$ , as no input to this function lies in the intermediate domain  $[\tau - 1 + e_{\text{bts}}, \tau - e_{\text{bts}}]$ . The choice of  $\tau$  is arbitrary, but can modify the probabilities of false positives and negatives. To minimize the probability of false positives, one should choose  $\tau = p'$ .

From a practical point of view, parameters should be set so as to make the classification step as efficient as possible: the relative width of the gap  $(1 - 2e_{\text{bts}})/(\max \mathcal{P}' - \min \mathcal{N}')$  should be as large as possible, while keeping  $e_{\text{comp}} + e_{\text{bts}}$  somewhat smaller than  $2^{\delta-1}$ . This suggests that prior to this discretization, the ciphertext should be rescaled to a modulus  $2^\delta$  which is as small as possible while keeping  $e_{\text{comp}} \ll 2^\delta$ , followed by a sufficiently precise bootstrap.

**3.3.2 Grouping everything together.** Finally, the  $\text{match}_{\text{db}}$  function can be obtained by evaluating an OR tree. For this purpose, we use the identity  $x \vee y = x + y - x \cdot y$  in a tree-like manner with depth  $\log(\rho n_{\text{db}})$ , possibly adding cleaning steps when the precision degrades [DMPS24]. Alternatively, one may add all the match values and evaluate an integer indicator function to turn nonzero values into 1 and send 0 to 0, as described in [MHP<sup>+</sup>25, Section 3.1].

## 4 Reducing the number of bootstraps

When used for a large database, the approach of Section 3 bootstraps a very large number of scores (one per rotated iris template and database entry). Given the bootstrap cost, this overwhelmingly dominates the overall cost (see Section 6.2). In particular, the bootstrapping cost exceeds by far the linear algebra cost. This section describes our main ingredient for rebalancing these costs, which we call *folding*. It consists of a lightweight classification (send negative scores to small values and positive scores to large ones) in such a way that we can combine several ciphertexts together before bootstrapping while retaining the relevant information.

### 4.1 Overview of folding

**4.1.1 A high-level view.** Folding (for scalars) rests on a polynomial  $f$  such that  $f(\mathcal{N}) \subset [-\alpha, \alpha]$  while  $f(\mathcal{P}) \geq \beta$ , for a small  $\alpha$  compared to  $\beta$ . If  $(x_i)_{1 \leq i \leq k}$  is a set of scores in  $\mathcal{N} \cup \mathcal{P}$  such that at most one  $x_i$  is not in  $\mathcal{N}$ , we define  $S = \sum_{i=1}^k f(x_i)$  and notice that

- if all  $x_i$ 's are in  $\mathcal{N}$ , then  $S \leq k\alpha$ ;
- if one  $x_i$  is in  $\mathcal{P}$ , then  $S \geq \beta - (k-1)\alpha$ .

For  $\alpha < \beta/(2k-1)$ , we have that  $k\alpha < \beta - (k-1)\alpha$ , which allows us to discriminate between these two options using only the value  $S$ . From the homomorphic point of view, we can thus compute  $S$ , bootstrap it, and classify the resulting value to 0 if the input is in  $[-k\alpha, k\alpha]$  and to 1 if the input is  $\geq \beta - (k-1)\alpha$ . In this setting, what we compute is no longer match nor  $\text{match}_{\text{db}}$  but a partial version of  $\text{match}_{\text{db}}$  that groups  $k$  values of match (with an OR) as a single one. This divides the number of bootstraps by  $k$ .

**4.1.2 Probabilistic folding.** We now make the further assumption that negative values are drawn from a probability distribution  $\mathcal{D}$ . We then define a folding polynomial as follows.

**Definition 4.1.** Given an integer  $k$  and two closed intervals  $\mathcal{N}_f$  and  $\mathcal{P}_f$  with  $\max \mathcal{N}_f < \min \mathcal{P}_f$ , we fix two reals  $p_1, p_2 \ll 1$  and define a  $(k, \mathcal{N}_f, \mathcal{P}_f)$ -folding polynomial as a polynomial  $f$  with

$$\Pr_{(x_0, \dots, x_{k-1}) \leftarrow \mathcal{D}^k} \left( \sum_{i=0}^{k-1} f(x_i) \notin \mathcal{N}_f \right) \leq p_1 ,$$

$$\Pr_{(x_0, \dots, x_{k-1}) \leftarrow \mathcal{D}^{k-1}} \left( \min_{x_0 \in \mathcal{P}} f(x_0) + \sum_{i=1}^{k-1} f(x_i) \notin \mathcal{P}_f \right) \leq p_2 .$$

Let  $\mathbf{v}_0, \dots, \mathbf{v}_{k-1}$  be vectors of scores of dimension  $N$ . We make the following *folding assumption*: for all  $0 \leq i < N$ , at most one vector  $\mathbf{v}_j$  has its  $i$ -th coordinate that is not drawn from  $\mathcal{D}$ .

If the  $\mathbf{v}_j$ 's satisfy the folding assumption, and  $f$  is a  $(k, \mathcal{N}_f, \mathcal{P}_f)$ -folding polynomial, we build the vector  $\mathbf{w} = \sum_{j=0}^{k-1} f(\mathbf{v}_j)$  where, for a vector  $\mathbf{u} = (u_i)_i$ , we let  $f(\mathbf{u})$  denote the vector  $(f(u_i))_i$ . Assuming that all the scores are either in  $\mathcal{P}$  or drawn from  $\mathcal{D}$ , the definition of a folding polynomial gives the following, for  $0 \leq i < N$ :

- If  $(\mathbf{v}_j)_i$  is drawn from  $\mathcal{D}$  for all  $j$ , then  $\Pr(V_i \in \mathcal{N}_f) \geq 1 - p_1$ ;
- If there is a  $j$  with  $(\mathbf{v}_j)_i \in \mathcal{P}$ , then  $\Pr(\mathbf{w}_i \in \mathcal{P}_f) \geq 1 - p_2$ .

The result of the iris recognition process is true for the query index  $i$  if and only if  $V_i \in \mathcal{N}_f$ ; we deduce that, in case of a genuine match, we return true with probability  $\geq 1 - p_2$  and, in the case of a non-match, we return false with probability  $\geq 1 - p_1$ .

### 4.2 Designing the folding polynomial

Given a target function  $t(x)$  and a nonnegative weight function  $w(x)$ , we use approximation in the  $L^2$ -sense, by choosing a positive integer  $d$  and finding the degree- $d$  polynomial  $f$  minimizing

$$\int_{x \in \mathbb{R}} w(x) \cdot (t(x) - f(x))^2 \, dx .$$

As a weight function, we choose a combination of a probability density function  $\tilde{\mathcal{D}}(x)$  derived from the distribution  $\mathcal{D}$  that models negative scores and of the indicator function  $\mathbb{1}_{\mathcal{P}}(x)$  of  $\mathcal{P}$ . In practice, we consider  $w_\alpha(x) = \alpha \mathcal{D}(x) + \mathbb{1}_{\mathcal{P}}(x)$ , with  $\alpha \gg 1$  to put more emphasis on constraining the behavior on the negative scores than on the positive scores. This unbalancedness is motivated by the addition of many negative scores.

In order to design a target function, we stress that the requirements for folding are very different in nature for the negative side and for the positive side: for the negative side, the folding condition suggests that the polynomial has to approximate the zero function in the best possible way; for the positive side, however, the folding condition only requires values away from 0, but does not prescribe a precise target function. In practice, we obtained better results by allowing the function to grow slightly in the positive side. An example of folding polynomial is given in Figure 5.

Given  $w$ ,  $t$  and  $d$ , the computation of  $f$  starts by deriving an orthonormal basis of polynomials  $f_0, \dots, f_d$  of degree  $\leq d$  for the inner product

$$\langle \varphi, \psi \rangle = \int_{x \in \mathbb{R}} \varphi(x) \psi(x) w(x) \, dx .$$

The folding polynomial is then obtained as  $f = \sum_{i=0}^d \langle f_i, t \rangle f_i$ ; this reduces the problem to integration and linear algebra tasks.

### 4.3 Ensuring the folding assumption

The folding assumption asserts that in a given slot, at most one vector contains a score which is not drawn from  $\mathcal{D}$ . Ensuring this assumption thus depends on the discrimination properties of the iris recognition system but also on the way the scores are organized among vectors.

The encrypted matrix-matrix multiplication algorithm of Section 2.3 returns a list of ciphertexts which correspond to encryptions

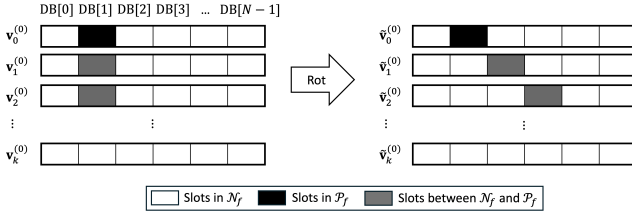


**Figure 1: Among  $k$  folding polynomial output ciphertexts of  $(v_r)_{r=1}^k$  for the same query eye, there is at most one matching DB entry. By rotating  $v_r$  by  $r$  positions, the folding assumption is fulfilled.**

of the columns of the underlying plaintext matrix-matrix multiplication. As such, and in view of the specification of the iris recognition task, the output of the CCMM step is a list of ciphertexts  $ct_r^{(\ell)} \in \mathcal{R}_Q^2$ , each containing in its  $i$ -th slot the score of matching the  $r$ -th rotation of the iris code against database entry  $i + \ell N$ , where  $0 \leq r < \rho$  and  $0 \leq \ell < n_{\text{db}}/N$ . We let  $v_r^{(\ell)}$  be the underlying vector of scores. We further assume that  $\rho < N$ .

We assume that the discrimination properties of the iris recognition system guarantee that when matching a fixed rotation of a given iris image to a set of pairwise distinct database entries (corresponding to different users), at most one of the resulting scores is not a negative one (hence not drawn from  $\mathcal{D}$ ). We define  $\tilde{v}_r^{(\ell)} = \text{Rot}_r(v_r^{(\ell)})$ ; then, the folding assumption is satisfied for the vectors  $\tilde{v}_r^{(\ell)}$ . Indeed, the  $i$ -th slot of  $\tilde{v}_r^{(\ell)}$  contains a score computing against the database entry of index  $\ell N + (i - r \bmod N)$ . These values are pairwise distinct for  $r < N$ , implying that the claim follows from our assumption on the discrimination properties of the iris recognition system. An illustration is provided in Figure 1.

#### 4.4 Description of the improved algorithm

With the above folding technique at hand, we can now describe our strategy for reducing the number of bootstraps. We focus on the main loop of Algorithm 1, which we improve as Algorithm 2.

The input intervals  $N_f$  and  $\mathcal{P}_f$  are like  $N'$  and  $\mathcal{P}'$  in Algorithm 1, but are set differently to take folding into account. The algorithm also takes as input a folding factor  $k$  and a folding polynomial  $f$ . Our folding strategy is split into two components: one just after CCMM, which uses  $f$ ; and the second one after a first classification. At this later stage, folded values drawn from  $\mathcal{D}$  have (with probability close to 1) been sent to values close to 0. Thanks to the folding assumption, in any given slot, at most one value is not close to 0; hence, we can simply add the corresponding values. Equivalently, the classification step acts as a second folding polynomial.

Bootstrapping is required prior to each call to a classification function, because of the depth consumption. The total number of bootstraps in Algorithm 1 was  $\approx 2\rho n_{\text{db}}/N$ , decomposed as  $\rho n_{\text{db}}/N$  to prepare the classification of scores,  $\rho n_{\text{db}}/N$  for the discretization, and a few more for the OR tree. In Algorithm 2, the number of bootstraps is  $\approx \rho n_{\text{db}}/(kN)$  before the classification, and a few more for the discretization and the OR tree. Overall, the number of bootstraps is reduced by a factor of  $\approx 2k$ .

---

#### Algorithm 2 Improved main loop using folding

---

**Require:** Same inputs as Algorithm 1, and parameters  $N_f$  and  $\mathcal{P}_f$ .  
**Require:** An intermediate folding amount  $k \leq \rho$  and a  $(k, N_f, \mathcal{P}_f)$ -folding polynomial  $f$ .  
 $(ct_r^{(\ell)})_{0 \leq r < \rho, 0 \leq \ell < n_{\text{db}}/N} \leftarrow \text{CCMM}(\widehat{\mathbf{M}_{\text{db}}}, \widehat{\mathbf{M}_{\text{qry}}})$   
 $ct_{\text{out}} \leftarrow (0, 0)$   
**for**  $0 \leq \ell < n_{\text{db}}/N$  **do**  
  **for**  $0 \leq r < \lceil \rho/k \rceil$  **do**  
     $ct_r^{(\ell)} \leftarrow (0, 0)$   
    **for**  $0 \leq r' < \min(k, \rho - rk)$  **do**  
       $s \leftarrow rk + r'$   
       $\mu_s^{(\ell)} \leftarrow \text{Ecd} \left( (\|\mathbf{m}_s^{(\text{qry})} \wedge \mathbf{m}_j^{(\text{db})}\|_1^{-1})_{N\ell \leq j < N(\ell+1)-1} \right)$   
       $ct_s^{(\ell)} \leftarrow ct_s^{(\ell)} \odot \mu_s^{(\ell)}$   
       $ct_r^{(\ell)} \leftarrow ct_r^{(\ell)} + \text{Rot}_s(f(ct_s^{(\ell)}))$   
    **end for**  
     $ct_r^{(\ell)} \leftarrow \text{Classify}_{\varepsilon_0, N_f, \mathcal{P}_f}(ct_r^{(\ell)})$   
     $ct_{\text{out}} \leftarrow ct_{\text{out}} + ct_r^{(\ell)}$   
  **end for**  
**end for**  
 $ct_{\text{out}} \leftarrow \text{BTS}(\text{Rescale}_{\Delta/2^\delta}(ct_{\text{out}}))$   
 $ct_{\text{out}} \leftarrow \text{Classify}_{\varepsilon_1, N', \mathcal{P}'}(ct_{\text{out}})$

---

This improvement does not come for free. The folding polynomial  $f$  needs to be evaluated on  $\rho n_{\text{db}}/N$  ciphertexts, and in order to be able to perform this evaluation before any bootstrap, the CCMM computation must take place at a higher modulus than before. Overall, bootstrap and classification costs drop, but linear algebra becomes more expensive and a new folding cost is incurred. We stress that even though it is almost transparent from an algorithmic perspective, increasing the linear algebra ciphertext modulus is challenging in practice (see Section 6).

## 5 System Design

So far, we focused on the algorithmic efficiency of homomorphic matching. In this section, we explain how to deploy it in a cryptographic protocol involving encryption and threshold decryption.

### 5.1 Iris recognition using ThFHE

We give an overview of the iris recognition system that we consider, based on threshold FHE (ThFHE).

**5.1.1 ThFHE.** ThFHE [AJLA<sup>+</sup>12, BGG<sup>+</sup>18] is an extension of FHE where the decryption key is secret-shared between  $n$  decryptors, so that at least  $t$  among them need to collaborate to decrypt and any subset of at most  $t - 1$  of them cannot recover any information on plaintexts underlying ciphertexts. More formally, a ThFHE scheme consists of four protocols with the following specifications.

- Key Generation is a distributed protocol between  $n$  decryptors; all decryptors have scheme parameters including the security level, the number  $n$  of decryptors and a threshold  $t$  as inputs; the protocol publicly outputs an encryption key  $\text{pk}$  and an evaluation key  $\text{evk}$ , and it outputs a decryption key share  $\text{sk}_i$  to the  $i$ -th party for all  $i \leq n$ ;

- Encryption is an algorithm that takes as inputs an encryption key  $pk$  and a plaintext  $\mu$ ; it outputs a ciphertext  $ct$ ;
- Evaluation is an algorithm that takes as inputs an evaluation key  $evk$ , a circuit  $C$  and ciphertexts  $(ct_j)_{1 \leq j \leq k}$  where  $k$  is the number of input wires of  $C$ , and outputs a ciphertext  $ct$ ;
- Decryption is a distributed 1-round protocol between  $t$  decryptors; all decryptors have the same ciphertext  $ct$  as input, the list of participating decryptors, and their own partial decryption key  $sk_{ij}$ ; the protocol publicly outputs a plaintext  $\mu$ . The algorithm run by the decryptors before communication is called partial decryption: at the end of it, the  $t$  decryptors publicly broadcast decryption shares  $(sh_{ij})_{1 \leq j \leq t}$ ; these are then combined by an algorithm called final decryption which may be run by any party and produces  $\mu$ .

For efficiency purposes, we assume that all decryptors involved during decryption are aware of who the other participating decryptors are. This is typically referred to as the synchronous setting, which was studied in [MBH23, MCPT24, CPS26].

Correctness posits that ciphertexts produced via encryptions and homomorphic evaluations decrypt to the plaintext evaluations of the same circuits on the plaintexts underlying the input ciphertexts. We refer to [BGG<sup>+</sup>18] for a formal definition.

Security is defined as follows. The adversary can corrupt  $c < t$  decryptors. This is assumed to occur at the outset of the game, which is referred to as selective security. Adaptive security allows the adversary to corrupt decryptors based on the ciphertexts and decryption key shares that it has viewed so far. We are not aware of any ThFHE scheme proved to be adaptively secure under standard assumptions, but: 1) we are not aware either of any adaptive attack on a ThFHE scheme that is selectively secure and 2) by a guessing argument, any selectively secure ThFHE scheme is adaptively secure with an  $(\frac{n}{t})$  factor amplification in the adversary's security advantage. Beyond decryptor corruptions, the adversary can adaptively make encryption queries on valid plaintexts, evaluation queries on ciphertexts created using encryption and evaluation queries, and partial decryption queries on these ciphertexts. Such partial decryption queries are allowed for at most  $t - c - 1$  decryptors for a given ciphertext. Security requires that the adversary's view can be simulated from publicly known data. We refer to [CPS26] for a formal definition.

As showed in [BGG<sup>+</sup>18], many FHE schemes can be readily converted in ThFHE schemes using the fact that decryption is essentially linear. This is notably the case of CKKS. If the key material generated by the key generation protocol is the same as in the base FHE scheme, then the ThFHE scheme performs evaluation by using the base FHE scheme and inherits its efficiency. The distributed key generation protocol from [MHP<sup>+</sup>25] is both efficient and provides keys that are almost the same as in CKKS. In this work, we use the extension of CKKS to a ThFHE scheme provided by [MHP<sup>+</sup>25] for key generation and [CPS26] for decryption.

**5.1.2 Iris recognition protocol.** The computation and communication flow of the ThFHE-based iris recognition protocol is as described in Figure 2. It involves four types of entities: queriers, computing servers, decryptors and a receiver.

At the outset, the decryptors run a distributed key generation: the encryption and evaluation keys  $pk, evk$  are made public and

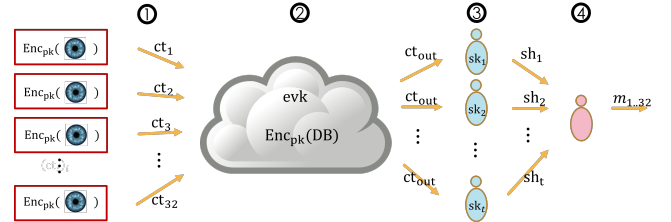


**Figure 2: Batch iris recognition based on ThFHE.** For the sake of simplicity, we do not depict the (plaintext) iris masks, nor potential zero-knowledge proofs required for active security.

respectively retrieved by the queriers and computing servers; each decryptor keeps its decryption key share  $sk_i$ . Second, the database of iris codes is encrypted (possibly using a different encryption format than provided by the encryption algorithm) and provided to the computing servers.

When a querier wants to match an individual against the database (Step 1 in the figure), the individual's iris codes (e.g., 31 of them per eye per user in the World ID scenario) are encrypted by the querier using  $pk$  and the resulting ciphertext is sent to the computing servers. The computing servers wait to batch many (32 in our case) such ciphertexts to increase throughput. Using  $evk$  and the encrypted database, they homomorphically perform the matching computation described in Section 2.1 (Step 2 in the figure). The output of this computation is a ciphertext encrypting bits (1 bit per querier) telling if there is a match or not. The corresponding ciphertext is then sent to the decryptors. At this point (Step 3 in the figure), each decryptor uses its decryption key share  $sk_i$  and  $t$  such decryptors engage in a decryption protocol. The decryption shares  $sh_i$  are sent to the receiver. Finally (Step 4 in the figure), the receiver runs the final decryption algorithm using the decryption shares  $sh_i$  to recover the plaintext output bits (1 bit per querier). Overall, the protocol comprises three communication rounds, and the communication is limited to the initial ciphertext, the ciphertext to be decrypted and the data sent to the receiver. This can be decreased to two rounds if the decryptors are identical to the computing servers, but we do not recommend this approach as it makes the computing servers entities that need strong protection. More rounds and larger amounts of communication can be considered in concrete deployment scenarios to distribute computations between computing servers and assess which decryptors are available.

**5.1.3 Security model.** In the basic security model, participants are all following the protocol and try to obtain any information beyond the fact that the queries produce matches or not. More concretely, an attacker is allowed to corrupt the computing server, the receiver and up to  $t - 1$  decryptors, and to make partial decryption queries as explained in the ThFHE security discussion. Given this view and all ciphertexts transmitted, it should not infer any information beyond the matching result, neither on the database iris codes nor the queried iris codes. Also, the attacker that also corrupts the querier should not learn anything about the database iris codes beyond what it can infer from the results of the queries. Reciprocally, an attacker that knows the database iris codes (for example because it built the database) should not learn anything on the queried iris

codes beyond what it can infer from the results of the queries. Such passive security is inherited from the security of the ThFHE scheme.

Protecting against active attackers (i.e., attackers that do not necessarily follow the protocol) can be achieved using zero-knowledge proofs. The weakest component against active attacks is decryption: indeed, the ThFHE final decryption from [BGG<sup>+</sup>18, CPS26] involves a linear combination  $b + \sum_{1 \leq j \leq t} sh_j$  of the decryption shares  $(sh_j)_{1 \leq j \leq t}$  produced by the decryptors and where  $b$  is part of the ciphertext to be decrypted; any participating decryptor can modify the output plaintext  $\mu$  to  $\mu + \mu'$  by adding (a scaled version of)  $\mu'$  to its share. Assuming that commitments of the decryption key shares  $sk_i$  are made public during key generation, an approach to prevent such an attack is to have the decryptor add a zero-knowledge proof that it genuinely built  $sh_j$  using its decryption key share  $sk_j$ . The statement to be proved is standard for lattice-based zero-knowledge proof systems (see, e.g., [LNP22]).

Additionally to strengthening decryption, one could add zero-knowledge proofs inside distributed key generation to force users to follow the protocol and zero-knowledge proofs for encryption to make sure the querier is following the protocol. Finally, one could require efficiently verifiable zero-knowledge proofs (SNARKs) that the computing servers performed their computations correctly. Although publicly verifiable FHE schemes exist, see [CCC<sup>+</sup>25] for a very recent reference specifically for CKKS, their proving time remains prohibitive. Instead, as the computation performed by the computing servers is public, adding computation redundancy seems to be a more practical approach.

## 5.2 Focus on the decryption protocol

Assume that the computing servers have obtained a ciphertext  $ct = (a, b)$  that decrypts to  $\mu \in \mathcal{R}$  that encodes bits in slots. Concretely, there exist a modulus  $q$ , a scale factor  $\Delta$  and a CKKS decryption key  $sk$  such that  $a \cdot sk + b = \Delta\mu + e \bmod q$  where  $\|e\|_\infty$  is small compared to  $\Delta$ . The decryption key is secret-shared as  $(sk_i)_{1 \leq i \leq n}$  among the  $n$  decryptors. In partial decryption [CPS26], the participating decryptors  $(i_1, \dots, i_t)$  compute

$$sh_{ij} = \lambda_j \cdot a \cdot sk_{ij} + e_{ij} + \sum_{1 \leq j' \leq t} \left( F_{k_{ij} k_{ij'}}(ct) - F_{k_{ij'} k_{ij}}(ct) \right),$$

where  $\lambda_j$  are secret-reconstruction coefficients,  $e_{ij}$  is a fresh noise term, and  $F$  is a pseudo-random function (such as AES or using the ring version of the Learning With Rounding problem [BPR12]) and user  $j$  knows the keys  $k_{ij} k_{ij'}$  and  $k_{ij'} k_{ij}$  for all  $j'$ . The final decryption algorithm consists in computing

$$b + \sum_{1 \leq j \leq t} sh_{ij} = b + a \cdot sk + \sum_{1 \leq j \leq t} e_{ij} = \Delta\mu + e + \sum_{1 \leq j \leq t} e_{ij}.$$

One then recovers  $\mu$  from  $\Delta\mu + e + \sum_j e_{ij}$  by rounding.

The noise term  $e_{ij}$  hides both the computation noise  $e$  and the decryption key shares  $sk_{ij}$ . In particular, because it is produced by homomorphic computations, the noise  $e$  may contain information on the secret key  $sk$  and the plaintexts occurring during the computation (including the queried and database iris scores). If this noise  $e$  is revealed, even partially, during decryption, then attacks can be mounted [LMSS22, PS24]. To hide  $e$ , the standard approach is to flood it with a much larger fresh noise [AJLA<sup>+</sup>12, BGG<sup>+</sup>18].

As detailed in [LMSS22], one can take  $e_{ij}$  with standard deviation  $\approx 2^{\lambda/2} \cdot B_e$ , where  $\lambda$  is the security parameter and  $B_e$  is a bound on  $\|e\|_\infty$ . As this is to hide a single scalar, the factor  $2^{\lambda/2}$  can be multiplied by  $N$  to hide a full ring element  $e$  (applying the triangle inequality to the statistical distance). With  $N \leq 2^{16}$  and  $\lambda = 128$ , this amounts to  $\log N + \lambda/2 \leq 80$  extra bits of noise on top of  $e$ . In turn, we need  $\Delta$  to be sufficiently large so that  $\mu$  can be recovered from  $\Delta\mu + e + \sum_j e_{ij}$  by rounding. Assuming that we limit the number of decryptors to  $t = 2^8$ , there should be a magnitude gap of  $\log N + \lambda/2 + \log t \leq 88$  bits between  $B_e$  and  $\Delta$ , to enable secure flooding while maintaining decryption correctness.

At the end of the homomorphic evaluation of the matching algorithm, the ciphertext may not be parameterized as above: the magnitude gap between  $B_e$  and  $\Delta$  is likely to be much smaller, e.g., of the order of 4 to 8 bits. To increase the gap, we homomorphically clean the message, using the technique from [CKSS25].

## 6 Implementation

We implemented our algorithm with folding (as described in Section 4) using the HEaaN2 library [Cry25]. HEaaN2 provides a high-performance GPU implementation of the CKKS scheme. Our (BTS and computing) parameter sets are summarized in Table 1. All our parameters yield 128-bit security according to the lattice estimator [APS15] and BTS failure probability below  $2^{-128}$ . As indicated, we use conjugate-invariant encoding as much as possible. Some conversion steps appear in the table when they cannot be fused with other steps, and hence use one level.

We used the ND-IRIS-0405 [BF16] iris image dataset and extracted its iris templates using Worldcoin’s open-source tool for plain iris recognition [AI23]. By matching (authentic) database entries against one another, we observed that the negative scores distribution  $\mathcal{D}$  can be approximated as the normal law of mean 0.008 and standard deviation 0.034. The number of distinct eyes in the dataset is smaller than our database size, so we generated iris codes and masks to fill the remaining database entries; the iris codes are sampled from a uniform binary distribution and masks are sampled from a Bernoulli distribution with parameter 0.8, assuming a moderately good image quality.<sup>2</sup>

Our proof-of-concept implementation considers a batch query of iris templates for 32 eyes (each one with 31 rotations), and compares them to a database of  $7 \cdot 2^{14}$  iris templates. The database is encrypted with 8 slices. One slice corresponds to the (shared)  $a$ -part of 7 ciphertext slices each one of which encrypts  $2^{14}$  templates, the 7 remaining slices corresponding to the  $b$ -parts of the ciphertexts. In a full deployment implementation, each slice would be stored by 1 GPU in a cluster of 8 GPUs (see Figure 3). The run-time performance is measured on a single NVIDIA RTX-5090 GPU, which is used to run the computation corresponding to any slice. This gives a reliable estimate for the computation times for the full database, but not for the communication costs between the 8 GPUs. In order to estimate these, we measured the timings on a cluster of 8 RTX-4090 GPUs with PCI-e links.

Due to space limitation, some aspects of the implementation are postponed to Appendix C. Here we focus on the linear algebra

<sup>2</sup>Although the actual behavior of iris templates is not simulated exactly, it does not affect the performance of our method.

**Table 1: CKKS Parameters.** The maximum RLWE modulus is denoted  $\log PQ$ ; the notation  $h$  ( $h'$ ) refers to the use of sparse secret encapsulation [BTPH22] with general secret key Hamming weight  $h$  and temporary weight  $h'$ ; Mult refers to non-bootstrapping levels and the notation “ $23 \times 20$ ” indicates the use 20 levels of 23-bit scaling factor.

(a) BTS Parameters

Part	Parameters	$\log N$	$\log PQ$	$h$ ( $h'$ )	$\log q_i$									dnum		
					Base	StC-first		FromCI	Mult	CtS-first			EvalMod	ToCI	CtS	
						StC	ToCI			StC	FromCI					
Preprocess	Half SI-BTS	16	1657	1024 (32)	33	-	20	23 $\times$ 20	-	52 $\times$ 8	36	36 $\times$ 3	3			
Core	CtS-first BTS								20	20 $\times$ 2	20					
Post-process	(Half)BTS	16	1719	1024 (32)	43	(25 $\times$ 2)	(25)	33 $\times$ 15	-	45 $\times$ 8	31	31 $\times$ 3	2			

(b) Computing Parameters

Part	Parameters	$\log N$	$\log PQ$	$h$	$\log q_i$							dnum
					Base	StC	FromCI	Mult				
Preprocess	Bit Extract & Clean	16	1050	1024	186 + 35 $\times$ 9 [masking + fromCI + clean + toCI + BE]							1
	Format Switch	13	212	512	23 $\times$ 6 + 24 $\times$ 2							8
Core	Query Encrypt	13	179	512	33	-	20	23 $\times$ 3 [fold] + 57 [ring pack]				-
	DB Encrypt	14	357	512	33	-	20	23 $\times$ 3 [fold] + 57 [ring pack] + 178 [CCMM]				-
	RingPack & Fold	16	251	32	33	-	20	23 $\times$ 3 [fold]				1
	Classify & Refold	16	1058	1024	43	26 $\times$ 2	25	33 [refold] + (35 $\times$ 3 + 30 $\times$ 4 + 30 $\times$ 4) [classify]				1
Post-process	Classify & Refold	16	1284	1024	43	25 $\times$ 2	25	(33 $\times$ 5) [refold] + (33 $\times$ 5 + 33 $\times$ 5) [classify]				1
	Clean	16	1058	1024	115 [output] + (123 + 92 + 52 + 72) [clean]							1

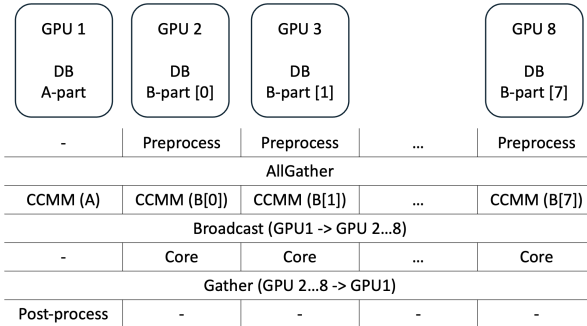


Figure 3: DB and Computation Distribution Over 8 GPUs

component, which is at the core of the computation and for which we considered several software and hardware accelerations.

## 6.1 Accelerating CCMM

Encrypted matrix multiplication is used to compute the numerators of the scores. We implemented the RGSW-based CCMM algorithm from [BCH<sup>+</sup>25] (see Section 2.3) using int8 cuBLAS matrix multiplication [NVI].

**6.1.1 RGSW-based CCMM with MSRLWE: database representation.** Following [BCH<sup>+</sup>25], we represent the database in MSRLWE-RGSW format. We pad the iris codes to dimension  $d = 2^{14}$  and use ring degree  $N_{\text{db}} = 2^{14}$  for database encryption and  $N'_{\text{qry}} = 2^{13}$  for query encryption. The MSRLWE-RGSW format then consists of a pair

of encryptions of  $\mathbf{M}_{\text{db}}$  and  $\mathbf{M}_{\text{db}} \cdot \mathbf{S}_{\text{qry}}$ , where  $\mathbf{S}_{\text{qry}}$  is a secret matrix derived from the secret keys used for the query encryption, represented as:

- $2^{14}$  (resp.  $2^{13}$ ) polynomials in  $\mathcal{R}_{2^{14}}$  for the  $a$ -part of  $\mathbf{M}_{\text{db}}$  (resp. for the  $a$ -part of  $\mathbf{M}_{\text{db}} \cdot \mathbf{S}_{\text{qry}}$ );
- $\ell \cdot 2^{14}$  (resp.  $\ell \cdot 2^{13}$ ) polynomials in  $\mathcal{R}_{2^{14}}$  for the  $b$ -part of  $\mathbf{M}_{\text{db}}$  (resp. for the  $b$ -part of  $\mathbf{M}_{\text{db}} \cdot \mathbf{S}_{\text{qry}}$ ).

If  $Q$  denotes the database ciphertext modulus, the total size of the encrypted database is thus  $3(\ell + 1)2^{27} \log Q$  bits.

**6.1.2 Fast PPMM using int8 cuBLAS.** The RGSW-based CCMM reduces encrypted matrix multiplication to four plaintext matrix multiplications modulo  $Q$ . These are performed using the cuBLAS library, which offers a primitive for products of two matrices with int8 coefficients with int32 output, using the int8 tensor cores of the RTX-5090. To use this primitive, matrix multiplication modulo  $Q$  is reduced to multiplication of int8 matrices. Following [BCH<sup>+</sup>25], we use a combination of two techniques:

- RNS representation, setting  $Q$  as a product of pairwise coprime small integers  $Q = q_1 \dots q_r$ , with  $q_i < 2^8$  for all  $i$ ; CCMM modulo  $Q$  then reduces to CCMM modulo  $q_i$ , which in turn reduces to four matrix multiplications modulo  $q_i$ ;
- Decomposition of a matrix  $M$  modulo an integer  $n^2$  (where  $n < 2^8$ ) under the form  $M + nM'$ ; then, using the identity  $(M + nM') \cdot (N + nN') = MN + n(M'N + MN') \bmod n^2$ , we reduce matrix multiplication modulo  $n^2$  to three matrix multiplications modulo  $n$ .

Our target modulus is  $Q \approx 2^{357}$ . When using int8 base arithmetic, the RNS representation approach is limited to a total modulus of

$\prod_{3 \leq p \leq 253} p^{\lfloor 8 \log 2 / \log p \rfloor} \approx 2^{354.83}$  (where the product is restricted to integers  $p$  that are prime): this falls just short. We thus use a combination of the two ideas, setting  $Q = \prod_{127 \leq p \leq 253} p^2$ : we reduce matrix multiplication modulo  $Q$  to matrix multiplication modulo  $p^2$  for each  $p$ , and then reduce each of the latter to three calls to int8 matrix multiplication. We note that this mixed method is more efficient than simple RNS in terms of memory representation. Even if the total modulus representable using RNS was large enough, we would need 53 int8 matrices to represent a matrix modulo  $Q$ , whereas our solution only requires 48, a saving of almost 10%.

**6.1.3 Database distribution and memory consumption.** As we represent a matrix modulo  $Q$  as 48 int8 matrices of the same dimension, the total size of the encrypted database is  $48 \cdot 3 \cdot (\ell + 1)2^{27}$  bytes. For  $\ell = 1$ , this is already 36GB, which is larger than the main memory of an RTX-5090 GPU. Instead, we note that the  $A$ -part of the result only depends on the  $A$ -part of the database, while the  $B$ -part of the result only depends on the  $B$ -part of the database. We thus choose a larger value of  $\ell$  and distribute the data over a computing node of 8 GPUs in the following way (see also Figure 3):

- one GPU stores the whole  $A$ -part of the representation of the database, which accounts for 18GB, and performs the computation of the  $A$ -part common to all scores;
- each one of the other 7 GPUs stores the  $B$ -part of ciphertexts corresponding to the iris codes of a slice of the database of  $2^{14}$  users, for 18GB, and computes the corresponding  $B$ -part of the scores.

This distribution allows each GPU to evaluate part of the CCMM in parallel. The  $A$ -part of the result, computed on the first GPU, is broadcast. The remaining GPUs can then complete the computation of the scores corresponding to their database slice.

## 6.2 Experimental results

Table 2 shows the runtime of each step within a single GPU, assuming parallel computation over 8 GPUs. The time is measured as the average over 100 runs. Excluding the communication between the ThFHE parties (see Section 5), it takes  $\approx 1.8$ s to compare 32 eyes against the encrypted database of  $7 \cdot 2^{14}$  iris codes.

**Table 2: Overall performance. Runtime is in ms, and the rows with a (\*) symbol correspond to communication steps between the GPUs.**

Component	Step	Runtime	Component	Step	Runtime
Core	CCMM	259	Post-process	Half SI-BTS	136
	Broadcast (*)	113		Extract & Clean	54
	Rotate	66		FormatSwitch	114
	RingPack	168		AllGather (*)	183
	Fold	261		Total	487
	CtS-first BTS	349		HalfBTS	8
	Classify	89		Classify	8
	Refold	14		Refold	1
	Gather (*)	1		BTS	12
	Total	1320		Clean	1
				Total	30

*Preprocessing.* Query preprocessing as a whole takes slightly less than 0.5s. The ring-switching operation is relatively expensive due to the use of a very large dnum. We stress that the target ring degree is forced by the CCMM RGSW algorithm, which prevents us for increasing the ring degree to reduce dnum.

The cost of the AllGather step could be reduced significantly by overlapping computation and communication, i.e., broadcasting parts of the queries while processing the next ones.

*Core.* A notable point in this component is that the folding strategy achieves its purpose of balancing costs between linear algebra and BTS. Using the naive strategy of Section 3 would remove the folding cost and decrease the CCMM and ring packing costs, as they would be executed with smaller ciphertext moduli. However, the number of ciphertexts to be bootstrapped would be 16 times higher: we can estimate this cost by multiplying that of ‘‘CtS-first BTS’’ in Table 2 by 16, leading to at least 5s. This is a crude estimate, as the computation involves other steps and BTS could be re-optimized.

Most of the ring packing time comes from the encoding of the plaintext masks, which cannot be pre-computed. The high cost of the folding step is due to its large number of inputs: 248 ciphertexts in ring degree  $N = 2^{16}$ , with a cost of  $\approx 1.05$  ms for each.

*Post-processing.* The cost for post-processing is almost negligible compared to the other components because it handles a single ciphertext. The resulting ciphertext has 88-bit of precision with a scaling factor of 105 bits over a modulus of 115 bits.

*ThFHE communications.* Table 2 does not show the communication between the ThFHE parties (querier, servers, decryptors and receiver). As described in Appendix C.1, the size of a ciphertext corresponding to a user’s query is 512KB (which may be lowered for a small increase of the servers’ runtime). The ciphertext sent by the servers to the decryptors can be represented in ring-degree  $2^{13}$ . Assuming a modulus of 128 bits (to enable flooding), this gives a ciphertext size of 256KB. In fact, only half of this (the  $a$ -part) is needed by the decryptors, whereas the  $b$ -part can be sent directly to the receiver. Each decryptor sends a decryption share of 128KB to the receiver. By observing that the  $b$ -part and decryption shares can be taken in a subring of dimension 32 (for a batch of 32 users) and truncated to a few bits, the total communication towards the receiver reduces to less than 1KB, so that only latency matters.

## 7 Conclusion

Our work demonstrates the relevance of ThFHE for large-scale privacy-preserving biometric recognition, offering similar efficiency as solutions based on secret-sharing MPC while having much milder requirements in terms of communication, and allowing a greater distribution of security and computation.

The folding technique allows one to aggressively reduce the amount of encrypted data at an early stage in large-scale FHE computations. We expect this idea to be useful in other settings.

Finally, regarding homomorphic algorithmic design, our work illustrates major efficiency progress on homomorphic linear algebra. It becomes so efficient that it can be worth sacrificing some efficiency on heavy linear algebra computations (by placing them at a higher modulus) in order to reduce the cost of calls to other more expensive homomorphic primitives, such as bootstrapping.

## Acknowledgments

We thank Isabelle Guérin-Lassous, Jaejin Lee, Daejun Park and Minje Park for helpful discussions.

## References

- [AB24] G. S. Arepalli and P. Boobalan. Privacy-preserving correlation-based multi-instance iris verification on malicious server using Cheon-Kim-Kim-Song fully homomorphic encryption. *J. Electron. Imaging*, 2024.
- [AI23] Worldcoin AI. IRIS: Iris recognition inference system of the Worldcoin project, 2023. Available at <https://github.com/worldcoin/open-iris>.
- [AJLA<sup>+</sup>12] G. Asharov, A. Jain, A. López-Alt, E. Tromer, V. Vaikuntanathan, and D. Wichs. Multiparty computation with low communication, computation and interaction via threshold FHE. In *EUROCRYPT*, 2012.
- [ALGRB23] R. Arjona, P. López-González, R. Román, and I. Baturone. Post-quantum biometric authentication based on homomorphic encryption and classic McEliece. *Applied Sciences*, 13, 2023.
- [APS15] M. R. Albrecht, R. Player, and S. Scott. On the concrete hardness of learning with errors. *J. Math. Cryptol.*, 2015. Software available at <https://github.com/malb/lattice-estimator> (commit 352ddaf4a288a0543f5d9eb588d2f89c7acec463).
- [BCH<sup>+</sup>24] Y. Bae, J. H. Cheon, G. Hanrot, J. H. Park, and D. Stehlé. Plaintext-ciphertext matrix multiplication and bootstrapping: fast and fused. In *CRYPTO*, 2024.
- [BCH<sup>+</sup>25] Y. Bae, J. H. Cheon, G. Hanrot, J. H. Park, and D. Stehlé. Fast homomorphic linear algebra with BLAS. 2025. Available at <https://arxiv.org/abs/2307.09288>.
- [BCKK25] Y. Bae, J. H. Cheon, M. Kang, and T. Kim. High-throughput AES transciphering using CKKS: less than 1ms. In *WAHC*, 2025.
- [BCKS24] Y. Bae, J. H. Cheon, J. Kim, and D. Stehlé. Bootstrapping bits with CKKS. In *EUROCRYPT*, 2024.
- [BF16] K. W. Bowyer and P. J. Flynn. The ND-IRIS-0405 iris image dataset, 2016. Available at <https://arxiv.org/abs/1606.04853>.
- [BGG<sup>+</sup>18] D. Boneh, R. Gennaro, S. Goldfeder, A. Jain, S. Kim, P. M. R. Rasmussen, and A. Sahai. Threshold cryptosystems from threshold fully homomorphic encryption. In *CRYPTO*, 2018.
- [BGK<sup>+</sup>24] R. Bloemen, B. Gillespie, D. Kales, P. Sippel, and R. Walch. Large-scale MPC: Scaling private iris code uniqueness checks to millions of users. IACR eprint, 2024. Available at <https://eprint.iacr.org/2024/705>.
- [BGV14] Z. Brakerski, C. Gentry, and V. Vaikuntanathan. (Leveled) fully homomorphic encryption without bootstrapping. *ACM Trans. Comput. Theory*, 2014.
- [BHVP24] A. Bassit, F. Hahn, R. N. J. Veldhuis, and A. Peter. Improved multiplication-free biometric recognition under encryption. *IEEE Trans. Biom. Behav. Identity Sci.*, 6, 2024.
- [BKSS24] Y. Bae, J. Kim, D. Stehlé, and E. Suvanto. Bootstrapping small integers with CKKS. In *ASIACRYPT*, 2024.
- [BPR12] A. Banerjee, C. Peikert, and A. Rosen. Pseudorandom functions and lattices. In *EUROCRYPT*, 2012.
- [Bra12] Z. Brakerski. Fully homomorphic encryption without modulus switching from classical gapSVP. In *CRYPTO*, 2012.
- [BTPH22] J.-P. Bossuat, J. Troncoso-Pastoriza, and J.-P. Hubaux. Bootstrapping for approximate homomorphic encryption with negligible failure-probability by using sparse-secret encapsulation. In *ACNS*, 2022.
- [BZC<sup>+</sup>23] P. Bauspiel, C.-M. Zok, A. Costache, C. Rathgeb, J. Kolberg, and C. Busch. MT-PRO: Multibiometric template protection based on homomorphic transciphering. In *WIFS*, 2023.
- [CCC<sup>+</sup>25] I. Cascudo, A. Costache, D. Cozzo, D. Fiore, A. Guimaraes, and E. Soria-Vazquez. Verifiable computation for approximate homomorphic encryption schemes. In *CRYPTO*, 2025.
- [CCKL16] J. H. Cheon, H. Chung, M. Kim, and K.-W. Lee. Ghostshell: Secure biometric authentication using integrity-based homomorphic evaluations. IACR ePrint, 2016. available at <http://eprint.iacr.org/2016/484>.
- [CGGI20] I. Chillotti, N. Gama, M. Georgieva, and M. Izabachène. TFHE: fast fully homomorphic encryption over the torus. *J. Cryptol.*, 2020.
- [CHK<sup>+</sup>18] J. H. Cheon, K. Han, A. Kim, M. Kim, and Y. Song. Bootstrapping for approximate homomorphic encryption. In *EUROCRYPT*, 2018.
- [CHK<sup>+</sup>21] J. Cho, J. Ha, S. Kim, B. Lee, J. Lee, J. Lee, D. Moon, and H. Yoon. Transciphering framework for approximate homomorphic encryption. In *ASIACRYPT*, 2021.
- [CKK20] J. H. Cheon, D. Kim, and D. Kim. Efficient homomorphic comparison methods with optimal complexity. In *ASIACRYPT*, 2020.
- [CKKS17] J. H. Cheon, A. Kim, M. Kim, and Y. Song. Homomorphic encryption for arithmetic of approximate numbers. In *ASIACRYPT*, 2017.
- [CKS<sup>+</sup>24] H. Choi, J. Kim, C. Song, S. S. Woo, and H. Kim. *Blind-Match*: efficient homomorphic encryption-based 1 : N matching for privacy-preserving biometric identification. In *CIKM*, 2024.
- [CKSS25] H. Choe, J. Kim, D. Stehlé, and E. Suvanto. Leveraging discrete CKKS to bootstrap in high precision. In *CCS*, 2025.
- [CPS26] F. Colin de Verdier, A. Passelègue, and D. Stehlé. On threshold fully homomorphic encryption with synchronized decryptrors. IACR eprint, 2026. Available at <https://eprint.iacr.org/2026/031>.
- [Cry25] CryptoLab. HEaaN2 library, 2025.
- [Dau04] J. Daugman. How iris recognition works. *IEEE Trans. Circuits Syst. Video Technol.*, 2004.
- [DMPS24] N. Drucker, G. Moshkowich, T. Pelleg, and H. Shaul. BLEACH: Cleaning errors in discrete computations over CKKS. *J. Cryptol.*, 2024.
- [EJB22] J. J. Engelsma, A. K. Jain, and V. Naresh Boddeti. HERs: homomorphically encrypted representation search. *IEEE Trans. Biom. Behav. Identity Sci.*, 4, 2022.
- [FV12] J. Fan and F. Vercauteren. Somewhat practical fully homomorphic encryption. IACR eprint, 2012. Available at <http://eprint.iacr.org/2012/144>.
- [ICDÖ23] A. Ibarrondo, H. Chabanne, V. Despiegel, and M. Önen. Grote: Group testing for privacy-preserving face identification. In *CODASPY*, 2023.
- [IKC<sup>+</sup>24] A. Ibarrondo, I. Kerenciler, H. Chabanne, V. Despiegel, and M. Önen. Monchi: Multi-scheme optimization for collaborative homomorphic identification. In *IH&MMSec*, 2024.
- [KN24] J. Kim and T. Noh. Modular reduction in CKKS. IACR eprint, 2024. Available at <http://eprint.iacr.org/2024/1638>.
- [KS18] D. Kim and Y. Song. Approximate homomorphic encryption over the conjugate-invariant ring. In *ISISC*, 2018.
- [LC25] M. López-García and E. F. Cantó-Navarro. Post-quantum authentication framework based on iris recognition and homomorphic encryption. *IEEE Access*, 13, 2025.
- [LLKN22] E. Lee, J.-W. Lee, Y.-S. Kim, and J.-S. No. Optimization of homomorphic comparison algorithm on RNS-CKKS scheme. *IEEE Access*, 2022.
- [LLNK22] E. Lee, J.-W. Lee, J.-S. No, and Y.-S. Kim. Minimax approximation of sign function by composite polynomial for homomorphic comparison. *IEEE Trans. Dependable Secur. Comput.*, 2022.
- [LMSS22] B. Li, D. Micciancio, M. Schultz, and J. Sorrell. Securing approximate homomorphic encryption using differential privacy. In *CRYPTO*, 2022.
- [LNP22] V. Lyubashevsky, N. K. Nguyen, and M. Plançon. Lattice-based zero-knowledge proofs and applications: Shorter, simpler, and more general. In *CRYPTO*, 2022.
- [LPR10] V. Lyubashevsky, C. Peikert, and O. Regev. On ideal lattices and learning with errors over rings. In *EUROCRYPT*, 2010.
- [MBH23] C. Mouchet, E. Bertrand, and J.-P. Hubaux. An efficient threshold access-structure for RLWE-based multiparty homomorphic encryption. *J. Cryptol.*, 2023.
- [MCPT24] C. Mouchet, S. Chatel, A. Pyrgelis, and C. Troncoso. Helium: Scalable MPC among lightweight participants and under churn. In *CCS*, 2024.
- [MHP<sup>+</sup>25] S. Min, G. Hanrot, J. H. Park, A. Passelègue, and D. Stehlé. Distributed key generation for efficient threshold-CKKS. IACR eprint, 2025. Available at <https://eprint.iacr.org/2025/2057>.
- [MPR20] M. K. Morampudi, M. V. N. K. Prasad, and U. S. N. Raju. Privacy-preserving iris authentication using fully homomorphic encryption. *Multim. Tools Appl.*, 79, 2020.
- [MPR21] M. K. Morampudi, M. V. N. K. Prasad, and U. S. N. Raju. Privacy-preserving and verifiable multi-instance iris remote authentication using public auditor. *Appl. Intell.*, 51, 2021.
- [MPVR21] M. K. Morampudi, M. V. N. K. Prasad, M. Verma, and U. S. N. Raju. Secure and verifiable iris authentication system using fully homomorphic encryption. *Comput. Electr. Eng.*, 89, 2021.
- [MSD23] M. K. Morampudi, M. Sandhya, and M. Dileep. Privacy-preserving bi-modal authentication system using fan-vercauteren scheme. *Optik*, 2023.
- [NVI] NVIDIA. cuBLAS library. <https://docs.nvidia.com/cuda/cublas/>. Accessed: 2026-01-13.
- [PM24] D. Palma and P. L. Montessoro. For your eyes only: A privacy-preserving authentication framework based on homomorphic encryption and retina biometrics. *IEEE Access*, 12, 2024.
- [PS73] M. Paterson and L. J. Stockmeyer. On the number of nonscalar multiplications necessary to evaluate polynomials. *SIAM J. Comput.*, 1973.
- [PS24] A. Passelègue and D. Stehlé. Low communication threshold fully homomorphic encryption. In *ASIACRYPT*, 2024.
- [SSTX09] D. Stehlé, R. Steinfeld, K. Tanaka, and K. Xagawa. Efficient public key encryption based on ideal lattices. In *ASIACRYPT*, 2009.
- [WOAS25] R. Weber, R. Orendorff, G. Almashaqbeh, and R. Solomon. Parasol compiler: Pushing the boundaries of FHE program efficiency. IACR eprint, 2025. Available at <https://eprint.iacr.org/2025/1144>.

## A More CKKS Background

### A.1 Bootstrapping flavors

CKKS bootstrapping comes in a number of flavors; we use the following ones:

- the original bootstrap [CHK<sup>+</sup>18], which we call “CtS-first”, starts with a ciphertext at the bottom modulus, and ends by the so-called “slot-to-coefficients step” (StC), which homomorphically converts the encoding of the ciphertext;
- the “StC-first” variant moves StC from the end to the beginning of the bootstrap, and requires that the latter starts at a higher modulus;
- when bootstrapping a coefficient-encoded ciphertext and expecting a slot-encoded output, the StC step can simply be discarded, giving what is called “Half bootstrapping” or Half-BTS [CHK<sup>+</sup>21];
- Dedicated solutions exist for the bootstrapping of ciphertexts encrypting vectors of small integer (SI-BTS) [BCKK25] (and Half-SI-BTS for its half-bootstrapping variant).

### A.2 Ring packing

The embedding from  $\mathcal{R}_{Q,N} = \mathbb{Z}[X]/\langle Q, X^N + 1 \rangle$  to  $\mathcal{R}_{Q,2^k N} = \mathbb{Z}[Y]/\langle Q, Y^{2^k N} + 1 \rangle$  defined by  $X \mapsto Y^{2^k}$ , can be used to map a ciphertext  $(a, b)$  from  $\mathcal{R}_{Q,N}$  to  $\mathcal{R}_{Q,2^k N}$ . When using the slot encoding, in terms of the underlying message, this corresponds to sending  $(x_i)_{0 \leq i < N/2}$  to  $(x_{i \bmod N/2})_{0 \leq i < 2^{k-1}N}$ . From this, we notice that  $2^k$  ciphertexts  $(ct_j)_{0 \leq j < 2^k}$  in  $\mathcal{R}_{Q,N}$  encrypted under the same secret key can be packed to a single ciphertext in  $\mathcal{R}_{Q',2^k N}$  by first embedding them, and then computing

$$\text{RingPack}\left(\left(ct_j\right)_{j=0}^{2^k-1}\right) = \sum_{j=0}^{2^k-1} \text{Mult}\left(ct_j, \text{Ecd}\left(\underbrace{0}_{jN/2}, \underbrace{1}_{(2^k-j-1)N/2}, \underbrace{0}_{N/2}\right)\right).$$

This computation uses one multiplicative level for masking, which is realized by a plaintext-ciphertext multiplication.

### A.3 Conjugate-invariant encoding

A modified version of CKKS uses the *conjugate-invariant* subring  $\mathcal{R}_{\text{CI}} = \mathbb{Z}[2 \cos(2\pi/N)]$  as plaintext space and  $\mathbb{R}^N$  as message space [KS18]: this provides  $N$  real-valued slots in contexts where one has no use for complex numbers. As our computations handle real numbers, we only use conjugate-invariant encoding. Some homomorphic primitives (bootstrapping, ring-switching), however, are more efficient using complex encoding. The conversions can be performed without decrypting [BCKK25] and will be denoted by ToCI and FromCI. They are cheap but consume one multiplicative level.

## B Classification functions

Several techniques have been developed for building classification functions, mostly in the context of evaluating comparisons. Two families of approaches can be considered.

- Use a composition of small degree polynomials; this consumes fewer homomorphic operations, but suffers from higher multiplicative depth and hence often more bootstraps [CKK20];

- Use a large degree polynomial constructed using the multi-interval Remez algorithm, and evaluated using the Paterson-Stockmayer algorithm [PS73]. This decreases multiplicative depth, but may lead to very large degrees and hence high costs.

These two methods are the two ends of a spectrum corresponding to a tradeoff between depth (or modulus consumption) and computational cost; as such, intermediate solutions have been considered, by composing medium-degree polynomials built using the multi-interval Remez algorithm [LLNK22, LLKN22]; we shall follow this approach. In order to build an  $(I_0, I_1, \epsilon)$ -classification function given a bound  $d$ , we use the multi-interval Remez algorithm to find a minimal  $\epsilon_0$  and a degree- $d$  polynomial  $P_0$  such that  $P_0$  is a  $(I_0, I_1, \epsilon_0)$ -classification function. Then, for  $Q \circ P_0$  to be an  $(I_0, I_1, \epsilon)$ -classification function, it suffices that  $Q$  is an  $([-\epsilon_0, \epsilon_0], [1 - \epsilon_0, 1 + \epsilon_0], \epsilon)$  classification function; we then use the same idea recursively, obtaining a sequence of  $\epsilon_j$ ’s, until  $\epsilon_j \leq \epsilon$ .

The cost of classification in CKKS is related both to the relative width of the gap between  $I_0$  and  $I_1$ , namely

$$\frac{\min(I_1) - \max(I_0)}{\max(I_1) - \min(I_0)}$$

and, in a more subtle manner, to the position of the gap (classification is easier if one of the intervals  $I_0$  or  $I_1$  is much smaller than the other one).

## C More details on the implementation

The detailed modulus consumption of the various steps is provided in Figure 4.

### C.1 Query preprocessing

Each query is initially packed in vectors with coordinates that are integers of  $\beta = 4$  bits. They are encrypted using a low ciphertext modulus  $q_{\text{pre}} = 2^{16}$  to optimize communication and BTS. We use the RLWE format with ring degree  $N = 2^{16}$  (the MSRLWE format with a smaller ring degree could be used to further reduce communication, at the expense of a ring-packing cost on the server side). For a query dimension  $d \leq 2^{14}$  and  $\rho = 31$  rotations, each query is encrypted as a pair of ciphertexts, for a total size of 512KB. The whole input thus consists of 62 ciphertexts, distributed over the 7 GPUs of our cluster. Each GPU processes its part of the query, all parts being broadcast after preprocessing in the AllGather step of Figure 3.

We use Half-SI-BTS followed by bit extraction as described in [BKSS24], using homomorphic parameters described in Table 1 part (a) for bootstrapping and part (b) for bit extraction. We then clean the ciphertexts to recover enough precision, and turn them into the bitmask format (see Section 2.1.3) via

$$\text{ct\_mask} = \text{Mult}(1 - 2 \cdot \text{ct}, m).$$

In order to prepare for CCMM, these ciphertexts are ring-switched to ring-degree  $2^{13}$ , each encrypting half a masked iris code. Each pair of half iris codes is converted to MSRLWE using format-conversion as in [BCH<sup>+</sup>24], and the scaling factor is reduced to the correct one for CCMM by modulus switching. In Table 2, we group these steps under the label “FormatSwitch”.

Ring-switching is performed in slots encoding. For this, we use masking to extract partial ciphertexts encrypting  $2^{13}$  consecutive

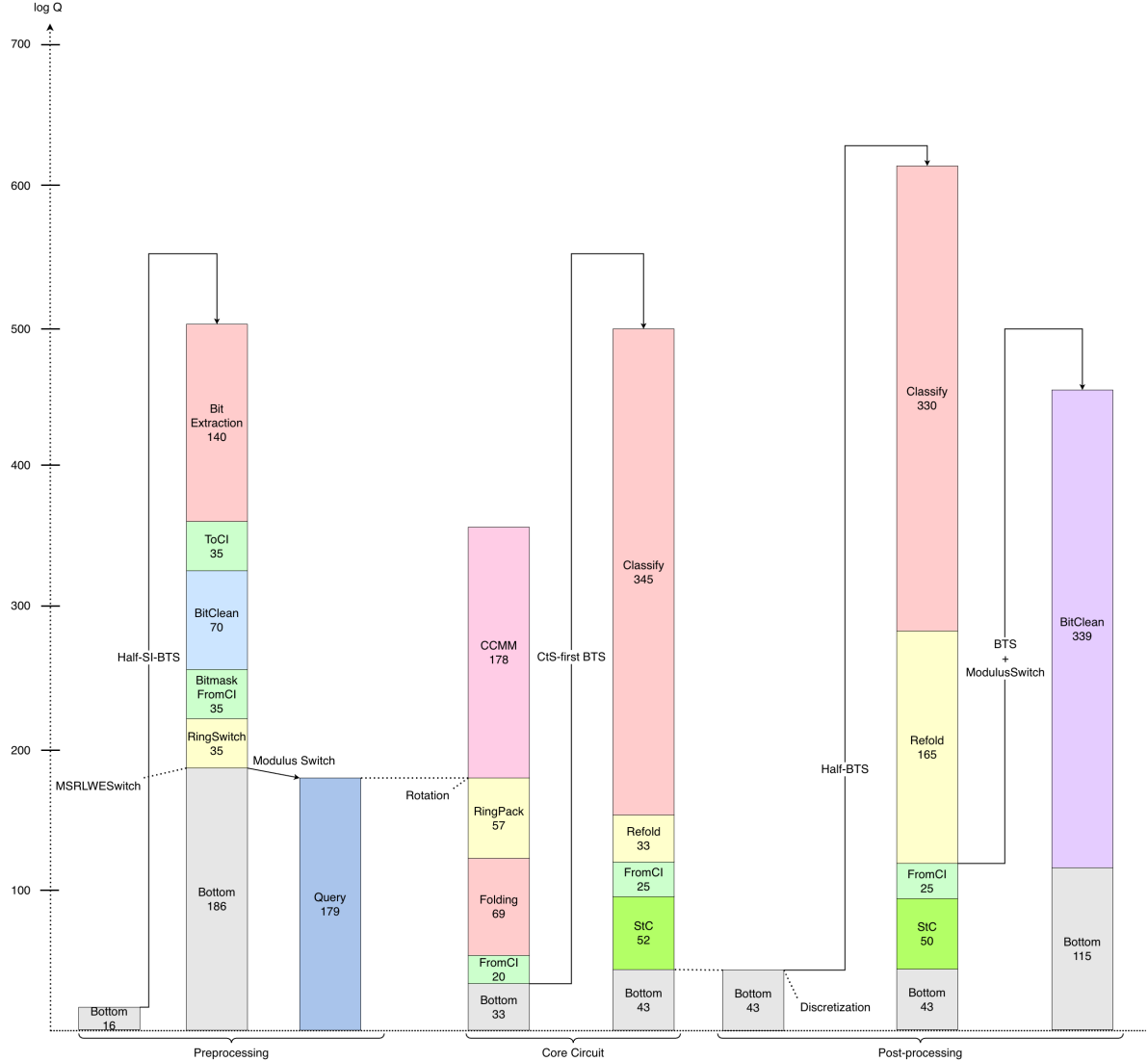


Figure 4: Modulus allocation

slots, then compute the trace (or, equivalently, partial rotate-and-sum) of each of these partial ciphertexts to bring the ciphertext down to the ring  $\mathcal{R}_{2^{13}}$ . The traces can be evaluated efficiently by first key-switching the partial ciphertext to a secret key in  $\mathcal{R}_{2^{13}}$ , and noticing that taking the trace of the ciphertext is then equivalent to taking the traces of the  $a$ -part and  $b$ -part, which corresponds to extraction of coefficients of degrees divisible by 8.

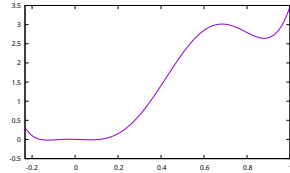
## C.2 Folding and bootstrapping

This part of the computation chain needs to handle a strong modulus constraint: the modulus  $Q$  used between CCMM and the modulus raising step of bootstrapping impact the total modulus  $Q^2/\Delta$  used for the database representation and, hence, the total database storage, which is a critical resource in our implementation.

Using the strategy of Section 4.2, we compute a folding polynomial  $P$  of degree 7 with folding capability  $k = 16$ . The evaluation of this polynomial requires 3 levels, for which we use a scaling factor of  $\Delta = 2^{23}$ . In order to retain as much precision as possible under this small scaling factor, we use secret key Hamming weight  $h = 32$  for this computation.

In order to construct the folding polynomial, we used target function  $x \mapsto (2 + x) \cdot \mathbb{1}_{\mathcal{P}}(x)$  (where  $\mathbb{1}_{\mathcal{P}}$  denotes the indicator function of  $\mathcal{P}$ ) and weight  $\alpha = 10^3$ . For the distribution  $\tilde{\mathcal{D}}$ , we considered the normal law with mean 0.008 and standard deviation 0.06. These parameters have been experimentally optimized. Folding operates on 16 values drawn from  $\mathcal{D}$  at once, leading to a larger occurrence of outlier values; for the design of the polynomial, using a distribution  $\tilde{\mathcal{D}}$  with larger standard deviation simulates

**Figure 5: Graph of the  $16 \times$  folding polynomial**



this larger occurrence of outliers. We obtain the polynomial

$$\begin{aligned} f(x) = & 106.553952 \cdot x^7 + 376.961251 \cdot x^6 - 412.746212 \cdot x^5 \\ & + 124.161550 \cdot x^4 + 24.347349 \cdot x^3 \\ & - 2.528271 \cdot x^2 - 0.173510 \cdot x + 0.004105 . \end{aligned}$$

Figure 5 displays the graph of  $f$  over  $[-0.233, 1]$ . We see that it takes values that are consistently very close to 0 around 0, and that large inputs have large but non-constant values.

In order to validate our folding design, we ran  $10^{12}$  folding experiments computing  $\sum_{0 \leq i < 16} P(X_i)$ ,  $\min_{x \in \mathcal{P}} P(x) + \sum_{0 \leq i \leq 14} P(Y_i)$  and  $\max_{x \in \mathcal{P}} P(x) + \sum_{0 \leq i \leq 14} P(Y_i)$  with  $X_i, Y_i$  independently drawn from  $\mathcal{D}$ . We found:

- 53 values coming from the sum of 16 values drawn from  $\mathcal{D}$  outside of  $[-0.13, 0.33]$ ;
- 542 values coming from the sum of 15 values drawn from  $\mathcal{D}$  and one value in  $\mathcal{P}$  outside of  $[0.4, 3.8]$ .

We take  $\mathcal{N}_f = [-0.13, 0.33]$  and  $\mathcal{P}_f = [0.4, 3.8]$  in Algorithm 2, and heuristically estimate the false negative probability as  $\approx 5.3 \cdot 10^{-11}$  and false positive probability as  $\approx 5.4 \cdot 10^{-10}$ . In order to account for the homomorphic evaluation error, we replace  $\mathcal{N}_f$  by  $\mathcal{N}'_f = [-0.15, 0.35]$ .

After evaluating the folding polynomial, we add the resulting ciphertexts, ring-pack to  $\log N = 16$  and bootstrap. This bootstrap is performed using the CtS-first variant, which starts by raising the modulus. The StC-first variant would lead to an increased database memory footprint.

### C.3 Classification and refolding

The classification steps are implemented using the general strategy outlined in Section 2.4; the input and output intervals for the classification step, and the degrees of the intermediate polynomials can be found in Table 3. The various scaling factors can be found in Table 1.

**C.3.1 Refolding.** The first folding folds only 16 values, even though the folding assumption holds for  $2^{14}$  values. To decrease the number of ciphertexts to be manipulated and communicated during the rest of the computation, we refold whenever possible to decrease the number of ciphertexts to a single one.

**C.3.2 Gathering.** In our experiment, 7 GPUs perform the folding computation and classification part of the algorithm; on a  $7 \cdot 2^{14}$  database for a batched query of 31 rotations of a 32 different iris images, each GPU handles 248 ciphertexts prior to folding, a number reduced to 16 after folding.

**Table 3: Classification functions**

Part	Input Intervals		Polynomials	
	$\mathcal{N}$	$\mathcal{P}$	Degree	Scale Factors
Core	[-0.15, 0.35]	[0.4, 3.8]	15	30 bits
			15	30 bits
			7	35 bits
Post-processing	[-0.414, 0.571]	[0.585, 1.414]	31	36 bits
			31	36 bits

In order to complete the folding after the first classification, these ciphertexts are sent to a single GPU, the latter handling the rest of the computation. In order to minimize the communication cost, we perform the StC part of the following bootstrap before gathering the ciphertexts, so that only HalfBTS has to be performed afterwards. The resulting communication costs appear as “Gather” in Table 2.

**C.3.3 Post-processing.** Post-processing outputs binary results that are packed into a single bit per query eye, with high enough precision to enable noise flooding (which is itself necessary for ThFHE security). The first step of the post-processing is a discretization to handle non-binary results. Given a coefficient-encoded input ciphertext, we rescale it to reduce its scaling factor to  $2^5$  (i.e., we set  $\delta = 5$ ), and bootstrap. This creates a gap between 0.571 and 0.585, which we use to classify as mentioned in Table 3. We conclude with high-precision cleaning as in [CKSS25].

### C.4 Scaling estimates

We discuss the scaling properties of our approach for a larger database, or for a larger or smaller query batch size.

**C.4.1 Handling a larger database.** In our experiments, database storage makes almost full use of the available GPU memory. Scaling up thus either requires increasing the amount of available hardware or move to hardware with other characteristics. For instance, running the experiment of [BGK<sup>+</sup>24], which handles a database of size  $2^{22}$ , would require 37 GPU clusters of the same type as the one that we consider (8 RTX-5090 GPUs). The cost of this configuration is comparable to that of the 24 H100 GPUs used in [BGK<sup>+</sup>24].

Scaling while keeping the same hardware would mean loading data from CPU memory after completing the CCMM step. This does not seem realistic: the next slice of  $7 \times 2^{14}$  entries of the database has size  $\approx 144\text{GB}$  and would require 5 to 7 seconds to transfer from main memory using the PCI bus. This is too large to significantly overlap with computation. In order to explore this direction, other hardware configurations have to be considered.

**C.4.2 Handling a larger batch size.** Handling larger query batch sizes is a different matter. For our batch of 32 query eyes, query size remains moderate and it is possible to increase it slightly within the available GPU RAM. For larger batch sizes, there is thus a tradeoff between scaling sequentially (by processing a large batch as several sequential smaller batches) or in parallel (by increasing the hardware configuration). For instance, the authors of [BGK<sup>+</sup>24] consider a batch of 32 users, but with 2 eyes per user. Compared to our experiments, this requires doubling the query batch size, which

we can handle in twice more time or in the same time by doubling the number of GPUs.

*C.4.3 Handling a smaller batch size.* Scaling down the query batch size does not allow a reduction in hardware configuration (because of the database storage), but yields faster processing time, at least down to 2 query eyes (which corresponds to handling a single

ciphertext per GPU after folding). For hardware reasons (smaller queries change the balance between compute-bound steps and memory-bound steps), we do not expect the scaling to be fully linear. For instance, we ran the core circuit on an 8 $\times$  smaller batch of 4 query eyes, and obtained a total time of 200ms for computational steps, so only a reduction of 6 $\times$ ; for such a batch, the end-to-end timing is of the order of 0.33s.